Title: Food resources shape bird assemblages, rendering trophic structure globally convergent

Authors list: Rubén Bernardo-Madrid[1-4*], Joaquín Calatayud[5,6], Kerry Stewart[7,8], Martin Rosvall[2], José Luis Tella[1], Chris Venditti[3], Luca Santini[9], Martina Carrete[10], Manuela González-Suárez[3]

Affiliations:

[1] Department of Conservation Biology, Doñana Biological Station, Consejo Superior de Investigaciones Cientificas (CSIC), Seville, Spain

[2] Integrated Science Lab, Department of Physics, Umeå University, Umeå, Sweden.

[3] Ecology and Evolutionary Biology Division, School of Biological Sciences, University of Reading, Reading RG6 6AJ, United Kingdom

[4] Department of Biogeography and Global Change, Museo Nacional de Ciencias Naturales (MNCN-CSIC), Madrid, Spain

[5] Departamento de Biología y Geología, Física y Química Inorgánica, Escuela Superior de Ciencias Experimentales y Tecnología (ESCET), Universidad Rey Juan Carlos, Madrid, Spain.

[6] Global Change Research Institute, Rey Juan Carlos University, Madrid, Spain

[7] K. Lisa Yang Center for Conservation Bioacoustics, Cornell University,

[8] Cornell Lab of Ornithology, Cornell University

[9] Department of Biology and Biotechnologies "Charles Darwin", Sapienza University of Rome, Piazzale Aldo Moro 5, Rome 00185, Italy

[10] Department of Physical, Chemical and Natural Systems, Universidad Pablo de Olavide, Seville, Spain.

* Corresponding author: r.bernardo.madrid@gmail.com

ABSTRACT

Species persist only when energy resources are available and organisms have traits to exploit them. Because resources such as fruit or carrion differ in abundance and diversity, general principles of energy flow and niche theory should shape differences in species richness among trophic guilds within assemblages. Yet, this hypothesis remains empirically untested. Here, we analyze 31,251 local bird surveys across North America and 10,753 large-scale assemblages worldwide. Within assemblages, more speciose guilds have more energy transformed into biomass, lower per-species energy demand, and greater morphological diversity associated with foraging strategies. These results help explain why, despite distinct ecological and evolutionary histories, the trophic structure of bird assemblages converges globally, suggesting that fundamental constraints related to food acquisition provide a blueprint for species assembly.

MAIN

Life depends on two fundamental constraints: food resources must be available, and organisms must possess the traits to acquire them. The effects of these constraints are well established at low levels of biological organization, determining whether individuals survive and whether populations and species persist or disappear (1-3). Yet how these constraints scale up to shape emergent properties of higher levels of biological organization, such as the structure and functioning of species assemblages, remain empirically uncertain.

Testing whether general principles of energy flow and niche partitioning shape species assemblages requires considering not only the number of species in an assemblage, but how those species are organized. Total species richness has long been linked to the total amount of energy available in the environment (4-6). Yet species are not interchangeable consumers of available energy (7-10), and food resources are not supplied in a single homogeneous form. Instead, food resources occur as distinct types — including fruits, leaves, animal prey and carrion — that are exploited by trophic guilds: species groups with distinct dietary requirements and ecological functions (7-11). Within a locality, resource types can differ in abundance and in the diversity of traits required to exploit them. Consequently, the amount and diversity of resource types should shape not only the overall richness of species assemblages, but also the relative representation of trophic guilds or the trophic structure of species assemblages. For example, more abundant resource types can support larger populations, reducing the risk of local extinction and allowing more species to persist (4, 5, 12-14; but see 15-17) (Fig. 1, left). Similarly, for any given amount of energy, species with lower energetic requirements per individual can have greater population abundances (2, 14, 18, 19) (Fig. 1, center). Complementarily, more heterogeneous resource types can require more distinct, and sometimes incompatible species traits, thereby favoring greater morphological diversity, specialization and niche partitioning (20-23) (Fig. 1, right). Although the availability of food resources and the traits to exploit them are fundamental constraints for all living organisms, many other aspects can also affect species richness, including biotic interactions, environmental filtering, historical processes, and stochastic dynamics (24-26). This raises an interesting question: to what extent do fundamental constraints operating on individuals shape emergent properties of complex ecological systems, such as the composition and trophic structure of species assemblages? Here, we show the strong association between the relative species richness of trophic guilds with proxy estimates of total resource biomass, species energetic demand, and niche partitioning across 31,251 local bird assemblages and 10,753 large-scale bird assemblages worldwide. This strong association helps explain the striking global convergence in trophic structure, supporting that fundamental processes to all living organisms act as guild assembly rules.

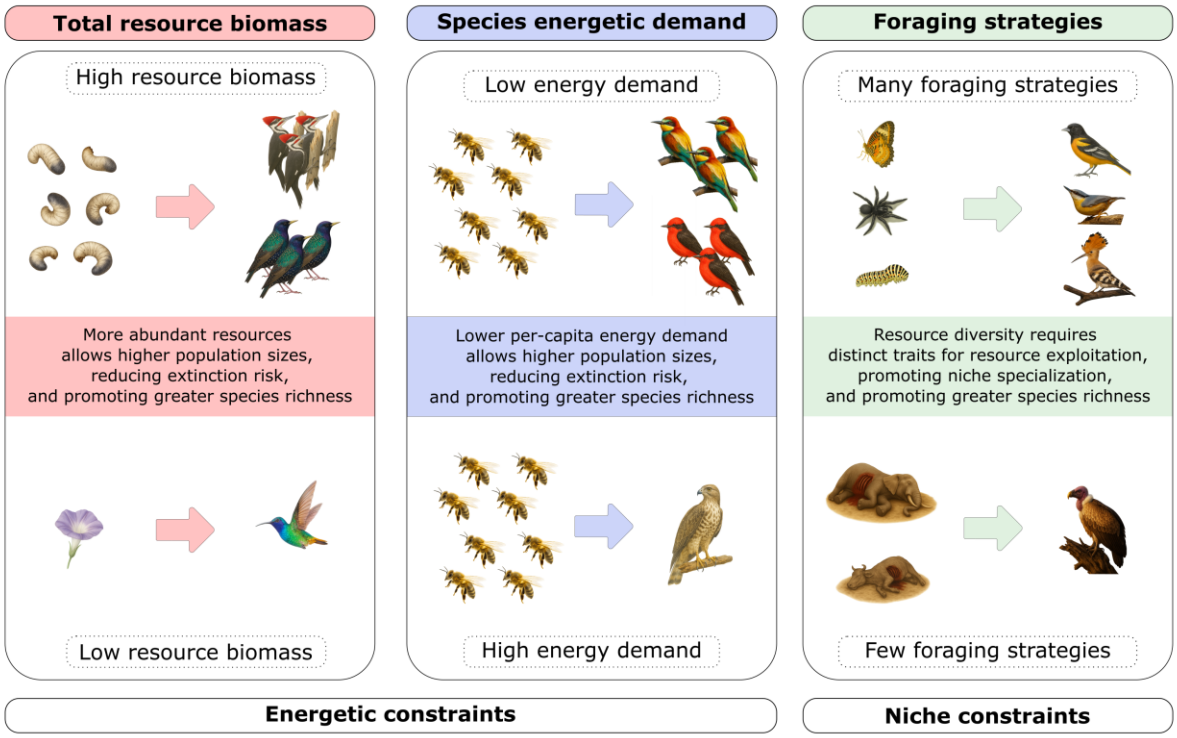

Fig. 1. Theoretical framework linking energetic and niche constraints to the relative richness of trophic guilds. Energetic constraints can shape guild richness through resource abundance and species energetic demand: more abundant resources can support larger populations, whereas lower per-capita energetic requirements can allow more individuals to persist for a given amount of resources. Niche constraints can shape guild richness through resource heterogeneity, which favors distinct foraging traits, specialization and niche partitioning.

RESULTS AND DISCUSSION

Local surveys in North America

Local-scale data supports a very strong imprint of energy and niche partitioning constraints on bird assemblage structure. Across 31,251 bird assemblages in the continental USA and Canada, defined from North American Breeding Bird Survey censuses (27), the relative species richness of trophic guilds was largely predicted by three variables reflecting: the amount of resource transformed into guild biomass (a proxy for total resource biomass (14)), the number of individuals sustained per unit biomass (capturing species energetic demand (2, 18, 28)), and the variance in foraging-related morphological traits (reflecting niche partitioning; $R^2_{marginal}$ of a linear mixed-effects model = 0.87). We defined trophic guilds as: omnivores, invertivores, vertivores, aquatic herbivores, terrestrial herbivores, aquatic predators, granivores, frugivores, nectarivores and scavengers (10). See Methods for further information on the variables and sensitivity analyses.

The individual effects of each predictor match the theoretical predictions (Fig. 1). More speciose guilds were associated with greater total guild biomass, more individuals per unit biomass, and broader morphological diversity related to foraging strategies (estimates ± s.e. = 0.219 ± 0.001, 0.187 ± 0.001 and 0.341 ± 0.001, respectively; all $p < 0.001$; Fig. 2). This pattern is illustrated

by the contrast between invertivores and scavengers. Invertivores were usually the most speciose group: they comprised many relatively small species (low species energetic demand), represented a large share of assemblage biomass and spanned diverse foraging morphologies associated with capturing prey in flight, on the ground, within vegetation, or beneath bark. Scavengers, by contrast, typically have fewer species, with larger individuals (higher energetic demand) and much more similar morphological traits for locating and consuming carrion.

Constraints related to the amount and diversity of available resources may be tightly coupled (of the 0.87 $R^2_{marginal}$ explained by the full model, 0.69 was shared among predictors rather than uniquely attributable to a single variable). Several non-exclusive mechanisms could generate this shared signal. First, greater resource abundance may bring rare or unreliable resources above the threshold needed to support specialist populations, thereby increasing exploitable niche diversity, functional partitioning and species co-occurrence (5). Second, greater resource abundance types may also be more structurally heterogeneous, providing a broader range of microhabitats and foraging opportunities leading to niche partitioning (13).

Despite the apparent coupling between resource quantity and resource diversity, the variance in morphological traits related to foraging strategies — our proxy for resource diversity and niche partitioning — made an important independent contribution (removing this predictor from the full model reduced the $R^2_{marginal}$ by 0.12, whereas removing total guild biomass or individuals per unit biomass reduced it by only 0.03). A complementary linear mixed-effects model further supported a role for morphological diversity beyond abundance-related processes (5). Morphological diversity remained strongly and positively associated with relative guild richness after accounting for differences in individual abundance among guilds ($p < 0.01$; $R^2_{marginal}$=0.54). See Methods for details.

Our results at local scale were consistent across 16 sensitivity analyses using alternative guild classifications and proxies, as well as controlling for sampling and statistical aspects (see Methods and supplementary text 1-10), suggesting a genuine ecological signal.

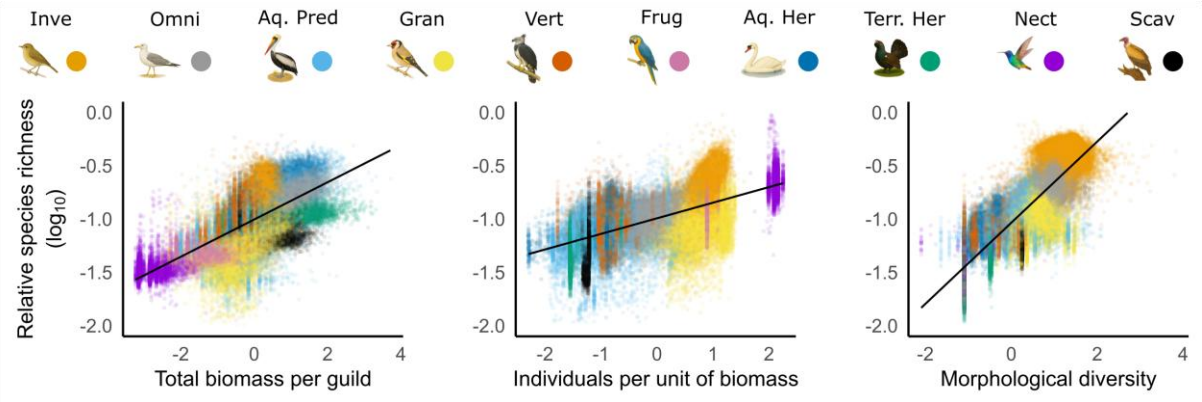

Fig. 2. Proxy estimates of resource amount and diversity largely predict the relative species richness of trophic guilds in 31,251 local-scale bird assemblages. Each point represents a bird guild in a census (guilds are color-coded). The y-axis shows the $\log_{10}$ relative

species richness. The x-axes show the three explanatory factors (scaled to a mean = 0 and SD = 1). Inve = Invertivores; Omni = Omnivores; Aq.Pred = Aquatic predators; Gran = Granivores; Vert = Vertivores; Frug = Frugivores; Aq.Her = Aquatic herbivores; Terr.Her = Terrestrial herbivores; Nect = Nectarivores; Scav = Scavengers.

Large-scale assemblages worldwide

A similar ecological signal emerged in large-scale bird assemblages worldwide. Across 10,753 large-scale assemblages, generated by overlaying global distribution maps of 8,648 bird species (29) onto equal-area grid cells of approximately 110 × 110 km (25, 30), variation in the relative species richness of the same ten guilds was largely explained by the same three ecological proxies tested at local scale ($R^2_{marginal}$ = 0.582). More speciose guilds had greater morphological diversity related to foraging strategies (estimate ± s.e. = 0.306 ± 0.001), greater total guild biomass (0.212 ± 0.001), and more individuals per unit biomass (0.073 ± 0.001; all $p < 0.001$). Morphological diversity was quantified using the same nine traits and procedure as at the local scale. In contrast, total guild biomass and individuals per unit biomass were calculated from global estimates of species density (31) weighted by the proportion of suitable habitat available to each species within each grid cell (see Methods). Our results were robust to uncertainty in density estimates, using alternative ecological predictors, and defining species assemblages at finer scale — grid cell and habitat combination (see sensitivity analyses in supplementary texts 11-14).

Large-scale analyses also supported partial coupling of mechanisms related to resource amount and resource diversity (5, 13). (shared variance = 0.409 of the total 0.582 $R^2_{marginal}$). As in the local analyses, morphological diversity was the stronger predictor ($\Delta R^2_{marginal}$ between the full model and a model without variance in morphological diversity = 0.135, while without total guild biomass = 0.034, and without individuals per unit biomass = 0.004).

Thus, analyses conducted at both local and broad spatial scales, using distinct definitions of bird assemblages and alternative proxies for resource availability and niche partitioning, converge on the same ecological signal: the relative representation of guilds within assemblages is strongly shaped by resource availability and by the morphological traits needed to exploit those resources (see sensitivity analyses in supplementary texts 1–14). Our results may point to a stronger contribution of niche processes than energetic processes to variation in relative species richness of guilds, consistent with studies showing that habitat heterogeneity can equal or exceed energy availability as a determinant of species-richness patterns (5, 13, but see 12). However, this inference remains tentative, because although the qualitative ecological signal was consistent across sensitivity analyses, the relative importance of morphological diversity (niche process) was reduced when accounting for expected relationship between species richness and morphological diversity (supplementary text 4).

A GLOBAL SIMILARITY IN THE TROPHIC STRUCTURE OF BIRD ASSEMBLAGES

Our local and large-scale analyses encompassed tens of thousands of bird assemblages that differ widely in species composition, richness and ecological, evolutionary and biogeographical

history. The strong signal across such heterogeneity suggests that the amount of resources and the diversity of traits required for its exploitation impose primary constraints on trophic structure, potentially acting as a blueprint for guild assembly upon which other factors known to shape species richness, including stochastic, historical, and biotic processes (24, 26, 32, 33) can exert more secondary and context-dependent roles. This hypothesis is consistent with long-standing assembly-rule theory and the related idea of guild proportionality, which predict that assemblages experiencing similar constraints should converge in the proportional representation of functional groups or guilds (8, 34, 35). In this way, our results provide empirical support for a mechanistic link between local resource-based processes and macroecological patterns, suggesting how previously reported regional variation in the trophic structure of terrestrial and marine assemblages (36-38) may emerge from spatial variation in food-resource regimes. For example, geographical variation in animal-dispersed fruits and floral resources may contribute to regional differences in the representation of frugivores and nectarivores (36-40). However, because major resources for birds, including plant material and invertebrates, are widespread and are a dominant food source in many ecosystems (41, 42), the same mechanisms can also drive a degree of global similarity among bird assemblages. Yet, the extent to which global convergence in trophic structure emerges, and how important it is relative to regional and local variation, remains unknown.

We find that the trophic structure of the 10,753 large-scale assemblages is strikingly similar (Fig. 3A). A single global profile, defined by the global mean proportion of species richness in each guild, explains ~74% of the trophic composition of all bird assemblages (Fig. 3A; $R^2_{marginal}$ from a linear mixed-effects model using the ten levels of guilds as predictors of the relative species richness of guilds). We also find secondary regional patterns, consistent with previous studies that found avian dietary guilds and diet strategies vary geographically and biogeographically (43, 44), and with broader evidence that community trophic structures are partly organized along climatic and environmental gradients (36-38). Hierarchical clustering analysis supported three regions broadly encompassing non-tropical, tropical, and extreme environments showing relatively small departures from the global profile (Fig. 3B). For instance, tropical assemblages show a slightly higher representation of fruit-eaters and nectar-feeders compared to non-tropical regions, consistent with a greater abundance and diversity of fleshy fruits, floral disparity and nectar in the tropics (39, 40). Yet a model allowing guild-specific means to vary among regions only modestly improved model fit ($\Delta R^2_{marginal} = 0.12$), supporting that regional differences are relatively minor compared with the dominant global structure. These results help explain the existence of both regional differences and global similarities, supporting that while regional patterns are ecologically meaningful (36-38, 43, 44), they may be considered as refinements upon a global pattern. Deviations from regional expectations in large-scale assemblages were only weakly associated with human footprint. Although statistically detectable, this association explained little additional variation in trophic structure ($\Delta R^2_{marginal} = 0.002$; estimate ± s.e.= −0.0053 ± 0.0002; $p < 0.001$; linear model including regional intercepts and human footprint per grid cell). This weak and negative relationship may suggest that contemporary assemblages partly reflect shifted regional baselines, where historical perturbations are already embedded in present-day trophic profiles, making

contemporary deviations difficult to interpret without explicit historical or reference baselines (45). Sensitivity analyses on the global profile using alternative dietary classification yielded similar results (supplementary text 15).

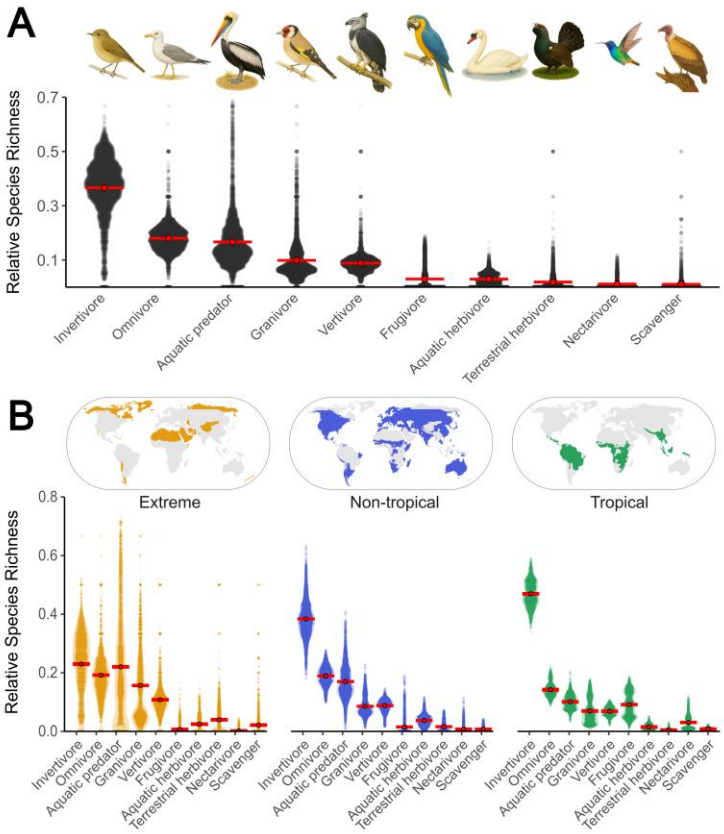

Fig. 3. Relative species richness across guilds is similar among bird assemblages worldwide. (A) Relative species richness of guilds across the 10,753 large-scale bird assemblages (each grey point is the observed relative species richness of a guild in one grid cell). The y-axis has been truncated for visualization, and a small number of points have been omitted (17 points in omnivores, three in granivores, and one in scavengers, all with relative species richness = 1). (B) Relative species richness of guilds in three geographical regions of the world largely distributed across non-tropical, tropical, and extreme environments. Red lines represent the 95% confidence intervals of the predicted values in the global (A) and regional (B) models.

CONTEXT AND OUTLOOK

For decades, ecological theory has suggested that energy availability, niche partitioning and guild assembly rules should shape species richness and community structure (4-6, 21, 22, 35). Yet the empirical importance of these mechanisms for the internal organization of assemblages has remained difficult to quantify. By combining these theoretical frameworks with global data on bird diet (9, 10), abundance (27), distributions (29) and foraging-related morphology (10, 23), we show that food-related constraints on individuals are strongly associated with the proportional representation of trophic guilds across tens of thousands of assemblages. This

signal supports the major role of energetic and niche processes in shaping the trophic structure of assemblages, while raising an important warning for biodiversity conservation: major shifts in resource regimes could restructure species assemblages (46), with potential impacts on ecosystem functioning (11, 23).

The strength and nature of our signal also speak to the long-debated question of whether ecological laws exist. Ecological systems may never be predicted by laws to the same extent as physical systems, because they are historically contingent and shaped by multiple interacting processes across temporal and spatial scales (47). Yet this does not imply unlimited possibilities for the structure and functioning of ecological systems (48). Across the planet, organisms face fundamental constraints including those related to energy acquisition (1-3). We show that these constraints narrow the range of configurations, assessed as trophic structures, that species assemblages can sustain. In this way, our results provide empirical support for deterministic constraints on the relative representation of species groups with distinct dietary requirements and ecological functions within assemblages, consistent with the existence of guild assembly rules (34, 35, but see 49). More broadly, our results offer a mechanistic explanation, and quantitative evidence, to the long-standing ecological perception that, when species identities are set aside, assemblages around the world tend to function in similar ways (8, 20).

As with any macroecological analysis, our results are constrained by data availability, requiring us to rely on ecological proxies and to focus on birds, a well-studied group. The consistency of the signal across distinct spatial scales, data sources, and analytical approaches, together with the fundamental role of the hypothesized mechanisms in living organisms, supports the robustness of our conclusions and their plausible extension to other taxa and multi-taxon assemblages. This extension is especially plausible for energetic processes. In other taxa, however, niche partitioning may remain important, but the relevant axes can be behavioral, spatial, or temporal rather than morphological (22, 50). Testing the broader applicability of our framework remains an important next step. For now, our study supports that while species number and identity may change from place to place, the trophic structure of assemblages appears to follow a simple logic that makes ecological systems easier to understand and predict.

References

1. R. L. Lindeman, The trophic-dynamic aspect of ecology. Ecology 23, 399–417 (1942).
2. J. H. Brown, J. F. Gillooly, A. P. Allen, V. M. Savage, G. B. West, Toward a metabolic theory of ecology. Ecology 85, 1771–1789 (2004).
3. S. A. L. M. Kooijman, Dynamic Energy Budget Theory for Metabolic Organisation (Cambridge Univ. Press, ed. 3, 2010).
4. D. H. Wright, Species–energy theory: An extension of species–area theory. Oikos 41, 496–506 (1983).
5. K. L. Evans, P. H. Warren, K. J. Gaston, Species–energy relationships at the macroecological scale: A review of the mechanisms. Biol. Rev. 80, 1–25 (2005).
6. B. A. Hawkins, E. E. Porter, J. A. F. Diniz-Filho, Productivity and history as predictors of the latitudinal diversity gradient of terrestrial birds. Ecology 84, 1608–1623 (2003).
7. R. B. Root, The niche exploitation pattern of the blue-gray gnatcatcher. Ecol. Monogr. 37, 317–350 (1967).
8. D. Simberloff, T. Dayan, The guild concept and the structure of ecological communities. Annu. Rev. Ecol. Syst. 22, 115–143 (1991).
9. H. Wilman, J. Belmaker, J. Simpson, C. de la Rosa, M. M. Rivadeneira, W. Jetz, EltonTraits 1.0: Species-level foraging attributes of the world's birds and mammals. Ecology 95, 2027 (2014).
10. J. A. Tobias et al., AVONET: Morphological, ecological and geographical data for all birds. Ecol. Lett. 25, 581–597 (2022).
11. Ç. H. Şekercioğlu, Increasing awareness of avian ecological function. Trends Ecol. Evol. 21, 464–471 (2006).
12. M. Pautasso, K. J. Gaston, Resources and global avian assemblage structure in forests. Ecol. Lett. 8, 282–289 (2005).
13. A. H. Hurlbert, Species–energy relationships and habitat complexity in bird communities. Ecol. Lett. 7, 714–720 (2004).
14. T. D. Meehan, W. Jetz, J. H. Brown, Energetic determinants of abundance in winter landbird communities. Ecol. Lett. 7, 532–537 (2004).
15. D. S. Srivastava, J. H. Lawton, Why more productive sites have more species: An experimental test of theory using tree-hole communities. Am. Nat. 152, 510–529 (1998).
16. K. L. Evans, N. A. James, K. J. Gaston, Abundance, species richness and energy availability in the North American avifauna. Glob. Ecol. Biogeogr. 15, 372–385 (2006).
17. D. Storch, E. Bohdalková, J. G. Okie, The more-individuals hypothesis revisited: The role of community abundance in species richness regulation and the productivity–diversity relationship. Ecol. Lett. 21, 920–937 (2018).
18. J. Damuth, Population density and body size in mammals. Nature 290, 699–700 (1981).
19. M. González-Suárez, A. Gonzalez-Voyer, A. von Hardenberg, L. Santini, The role of brain size on mammalian population densities. J. Anim. Ecol. 90, 653–661 (2021).
20. C. S. Elton, Animal Ecology (Macmillan, 1927).
21. J. M. Chase, M. A. Leibold, Ecological Niches: Linking Classical and Contemporary Approaches (Univ. of Chicago Press, 2003).

22. P. Chesson, Mechanisms of maintenance of species diversity. Annu. Rev. Ecol. Syst. 31, 343–366 (2000).
23. A. L. Pigot, C. Sheard, E. T. Miller, T. P. Bregman, B. G. Freeman, U. Roll, N. Seddon, C. H. Trisos, B. C. Weeks, J. A. Tobias, Macroevolutionary convergence connects morphological form to ecological function in birds. Nat. Ecol. Evol. 4, 230–239 (2020).
24. S. P. Hubbell, The Unified Neutral Theory of Biodiversity and Biogeography (Princeton Univ. Press, 2001).
25. R. Bernardo-Madrid, M. González-Suárez, M. Rosvall, M. Rueda, E. Revilla, M. Carrete, J. L. Tella, J. Astigarraga, J. Calatayud, A general rule on the organization of biodiversity in Earth's biogeographical regions. Nat. Ecol. Evol. 9, 1193–1204 (2025).
26. J. Calatayud et al., Positive associations among rare species and their persistence in ecological assemblages. Nat. Ecol. Evol. 4, 40–45 (2020).
27. D. Ziolkowski, M. Lutmerding, W. B. English, V. I. Aponte, M. R. Hudson, North American Breeding Bird Survey Dataset 1966–2022. U.S. Geological Survey data release (2023). doi:10.5066/P9GS9K64.
28. S. Nee, A. F. Read, J. J. D. Greenwood, P. H. Harvey, The relationship between abundance and body size in British birds. Nature 351, 312–313 (1991).
29. BirdLife International, Bird species distribution maps of the world. BirdLife International Data Zone (2021).
30. R. Bernardo-Madrid, J. Calatayud, M. González-Suárez, M. Rosvall, M. Rueda, E. Revilla, M. Carrete, J. L. Tella, Human activity is a major driver of species range expansion. Nat. Ecol. Evol. 3, 1112–1119 (2019).
31. L. Santini, V. Y. Mendez Angarita, C. Karoulis, D. Fundarò, N. Pranzini, C. Vivaldi, T. Zhang, A. Zampetti, S. J. Gargano, D. Mirante, L. Paltrinieri, TetraDENSITY 2.0—A database of population density estimates in tetrapods. Glob. Ecol. Biogeogr. 33, e13929 (2024).
32. M. Vellend, Conceptual synthesis in community ecology. Q. Rev. Biol. 85, 183–206 (2010).
33. J. J. Wiens, M. J. Donoghue, Historical biogeography, ecology and species richness. Trends Ecol. Evol. 19, 639–644 (2004).
34. B. J. Fox, The genesis and development of guild assembly rules. In E. Weiher, P. Keddy, Eds., Ecological Assembly Rules: Perspectives, Advances, Retreats (Cambridge Univ. Press, 1999), pp. 23–57.
35. J. B. Wilson, Guild proportionality: The elements of community structure. Oikos 56, 508–513 (1989).
36. M. Mendoza, M. B. Araújo, Climate shapes mammal community trophic structures and humans simplify them. Nat. Commun. 10, 5197 (2019).
37. M. Mendoza, M. B. Araújo, Trophic diversity is structured geographically in global mammal assemblages. Proc. Natl. Acad. Sci. U.S.A. 119, e2107560119 (2022).
38. J. D. González-Trujillo et al., Projecting community trophic structures for the last 120 000 years. Ecography 2025, e06899 (2025).
39. M. A. Sinnott-Armstrong, A. E. Downie, S. Federman, A. Valido, P. Jordano, M. J. Donoghue, Global geographic patterns in the colours and sizes of animal-dispersed fruits. Glob. Ecol. Biogeogr. 27, 1339–1351 (2018).

40. M. Chartier et al., Global patterns and a latitudinal gradient of flower disparity: Perspectives from the angiosperm order Ericales. New Phytol. 230, 821–831 (2021).
41. Y. M. Bar-On, R. Phillips, R. Milo, The biomass distribution on Earth. Proc. Natl. Acad. Sci. U.S.A. 115, 6506–6511 (2018).
42. Y. Rosenberg, Y. M. Bar-On, A. Fromm, M. Ostikar, A. Shoshany, O. Giz, R. Milo, The global biomass and number of terrestrial arthropods. Sci. Adv. 9, eabq4049 (2023).
43. W. D. Kissling, Ç. H. Şekercioğlu, W. Jetz, Bird dietary guild richness across latitudes, environments and biogeographic regions. Glob. Ecol. Biogeogr. 21, 328–340 (2012).
44. J.-Y. Barnagaud, N. Mazet, F. Munoz, M. Grenié, P. Denelle, M. Sobral, W. D. Kissling, Ç. H. Şekercioğlu, C. Violle, Functional biogeography of dietary strategies in birds. Glob. Ecol. Biogeogr. 28, 1004–1017 (2019).
45. A. Gonzalez, B. J. Cardinale, G. R. H. Allington, J. Byrnes, K. A. Endsley, D. G. Brown, D. U. Hooper, F. Isbell, M. Loreau, M. I. O'Connor, Estimating local biodiversity change: A critique of papers claiming no net loss of local diversity. Ecology 97, 1949–1960 (2016).
46. M. Mendoza, M. B. Araújo, Trophic reorganization of animal communities under climate change. J. Biogeogr. 52, doi:10.1111/jbi.15105 (2025).
47. J. H. Lawton, Are there general laws in ecology? Oikos 84, 177–192 (1999).
48. S. Linquist, T. R. Gregory, T. A. Elliott, B. Saylor, S. C. Kremer, K. Cottenie, Yes! There are resilient generalizations (or "laws") in ecology. Q. Rev. Biol. 91, 119–131 (2016).
49. L. Götzenberger et al., Ecological assembly rules in plant communities—approaches, patterns and prospects. Biol. Rev. 87, 111–127 (2012).
50. T. W. Schoener, Resource partitioning in ecological communities. Science 185, 27–39 (1974). doi:10.1126/science.185.4145.27.
51. J. R. Sauer, D. K. Niven, K. L. Pardieck, D. J. Ziolkowski Jr., W. A. Link, Expanding the North American Breeding Bird Survey analysis to include additional species and regions. J. Fish Wildl. Manag. 8, 154–172 (2017).
52. D. Lepage, Avibase—the world bird database. Bird Studies Canada (2024).
53. IUCN, The IUCN Red List of Threatened Species (2024).
54. W. Gearty, S. Chamberlain, rredlist: IUCN Red List Client, version 0.7.1 (2022).
55. L. Oksanen, S. D. Fretwell, J. Arruda, P. Niemelä, Exploitation ecosystems in gradients of primary productivity. Am. Nat. 118, 240–261 (1981).
56. G. A. Polis, D. R. Strong, Food web complexity and community dynamics. Am. Nat. 147, 813–846 (1996).
57. J. Cebrian, Patterns in the fate of production in plant communities. Am. Nat. 154, 449–468 (1999).
58. M. L. Pace, J. J. Cole, S. R. Carpenter, J. F. Kitchell, Trophic cascades revealed in diverse ecosystems. Trends Ecol. Evol. 14, 483–488 (1999).
59. J. B. Shurin, E. T. Borer, E. W. Seabloom, K. Anderson, C. A. Blanchette, B. Broitman, S. D. Cooper, B. S. Halpern, A cross-ecosystem comparison of the strength of trophic cascades. Ecol. Lett. 5, 785–791 (2002).
60. J. A. Estes et al., Trophic downgrading of planet Earth. Science 333, 301–306 (2011).
61. M. J. Coe, D. H. M. Cumming, J. Phillipson, Biomass and production of large African herbivores in relation to rainfall and primary production. Oecologia 22, 341–354 (1976).

62. S. J. McNaughton, M. Oesterheld, D. A. Frank, K. J. Williams, Ecosystem-level patterns of primary productivity and herbivory in terrestrial habitats. Nature 341, 142–144 (1989).
63. M. Mönkkönen, J. T. Forsman, F. Bokma, Energy availability, abundance, energy-use and species richness in forest bird communities: A test of the species–energy theory. Glob. Ecol. Biogeogr. 15, 290–302 (2006).
64. K. A. Nagy, Field metabolic rate and body size. J. Exp. Biol. 208, 1621–1625 (2005).
65. A. E. McKechnie, R. P. Freckleton, W. Jetz, Phenotypic plasticity in the scaling of avian basal metabolic rate. Proc. Biol. Sci. 273, 931–937 (2006).
66. L. A. Hordley, S. Gillings, O. L. Petchey, J. A. Tobias, T. H. Oliver, Diversity of response and effect traits provides complementary information about avian community dynamics linked to ecological function. Funct. Ecol. 35, 1938–1950 (2021).
67. J. Lefcheck, piecewiseSEM: Piecewise structural equation modeling in R. R package and online book (2021).
68. S. Nakagawa, H. Schielzeth, A general and simple method for obtaining R2 from generalized linear mixed-effects models. Methods Ecol. Evol. 4, 133–142 (2013).
69. P. Breheny, W. Burchett, Visualization of regression models using visreg. R J. 9, 56–71 (2017).
70. D. Bates, M. Maechler, B. Bolker, S. Walker, Fitting linear mixed-effects models using lme4. J. Stat. Softw. 67, 1–48 (2015).
71. K. Bartoń, MuMIn: Multi-Model Inference, version 1.47.5 (2023).
72. M. Jung, P. R. Dahal, S. H. M. Butchart, P. F. Donald, X. De Lamo, M. Lesiv, V. Kapos, C. Rondinini, P. Visconti, A global map of terrestrial habitat types. Sci. Data 7, 256 (2020).
73. J. H. Ward Jr., Hierarchical grouping to optimize an objective function. J. Am. Stat. Assoc. 58, 236–244 (1963).
74. P. J. Rousseeuw, Silhouettes: A graphical aid to the interpretation and validation of cluster analysis. J. Comput. Appl. Math. 20, 53–65 (1987).
75. M. Charrad, N. Ghazzali, V. Boiteau, A. Niknafs, NbClust: An R package for determining the relevant number of clusters in a data set. J. Stat. Softw. 61, 1–36 (2014).
76. H. Mu et al., An annual global terrestrial Human Footprint dataset from 2000 to 2018. Figshare (2024). doi:10.6084/m9.figshare.16571064.
77. M. Greenacre, Compositional data analysis. Annu. Rev. Stat. Appl. 8, 271–299 (2021).
78. O. L. Petchey, K. J. Gaston, Functional diversity (FD), species richness and community composition. Ecol. Lett. 5, 402–411 (2002).
79. S. Villéger, N. W. H. Mason, D. Mouillot, New multidimensional functional diversity indices for a multifaceted framework in functional ecology. Ecology 89, 2290–2301 (2008).
80. N. J. Gotelli, R. K. Colwell, Quantifying biodiversity: Procedures and pitfalls in the measurement and comparison of species richness. Ecol. Lett. 4, 379–391 (2001).
81. D. R. Roberts et al., Cross-validation strategies for data with temporal, spatial, hierarchical, or phylogenetic structure. Ecography 40, 913–929 (2017).
82. J. B. Grace, Structural Equation Modeling and Natural Systems (Cambridge Univ. Press, 2006).

83. W. R. Tobler, A computer movie simulating urban growth in the Detroit region. Econ. Geogr. 46, 234–240 (1970).

DATA AVAILABILITY

This study is based on publicly available and third-party datasets. Full details of data sources and access conditions are provided in the Methods. Third-party datasets should be obtained from the original providers under their respective terms of use.

COMPETING INTERESTS

The authors declare no competing interests.

ETHICS STATEMENT

This study did not involve new animal capture, handling or experimental procedures. Analyses were based on existing observational, trait, distributional and environmental datasets.

FUNDING

R.B.-M. was supported by the Junta de Andalucía, Consejería de Universidad, Investigación e Innovación, through the postdoctoral researcher contract programme of the Andalusian Knowledge System, EIDIA Horizonte 2027, grant DGP_POST_2024_00925, and an Olle Engkvist Foundation grant (220-0175). M. Rosvall was supported by the Swedish Research Council under grant 2023-03705. This research was also funded by the Spanish Ministry of Science and Innovation (MICINN) through the European Regional Development Fund (SUMHAL, LIFEWATCH-2019-09-CSIC-13, POPE 2014–2020) and the Ministry of Universities through the University of Seville, as part of the call for the Requalification of the Spanish University System 2021–2023, funded by the European Union's NextGenerationEU.

ACKNOWLEDGEMENTS

We thank Ana Benítez-López's lab for their insightful discussions.

MATERIAL AND METHODS

BBS routes in North America: Defining bird assemblages and their trophic structure

We defined local bird assemblages using abundance surveys recorded along standardized routes available on the North American Breeding Bird Survey (BBS) dataset (27). This dataset comprises thousands of roadside routes across the continental United States and Canada. Each BBS route is approximately 39 km long and comprises 50 fixed stops separated by about 0.8 km. At each stop, a single trained observer conducts a 3-minute point count, recording all birds seen within a 400 m radius and all birds heard. Although routes were intended to be surveyed once per breeding season, coverage varied among routes and years, and not all routes were run annually (27). We defined local assemblages at the route–year level, with species abundance calculated as the sum of detections across the 50 stops. We retained only surveys conducted under the standard BBS protocol (RunProtocolID/RPID = 101) following BBS data-use guidance and the official BBS data-release documentation (27). We further excluded taxa with consistently low detectability under the survey conditions (early-morning roadside point counts), including owls (Strigiformes), nightjars (Caprimulgiformes), shorebirds (Charadriiformes), and aquatic birds (27, 51). Because BBS data represent single-visit snapshots of local assemblages across a continent, they inevitably reflect transient environmental and biotic conditions at the time of sampling, including weather, migratory timing and the stage of the breeding cycle, as well as variation in detectability among observers. This heterogeneity is expected to increase spatiotemporal variance in species' counts and occurrences, reducing power to detect general signals. Thus, the results we report likely reflect patterns robust enough to emerge despite these sources of noise. Although differential detectability among species may affect local detection-based richness estimates, the main signal was retained after standardizing guild richness to the same number of detected individuals using individual-based rarefaction, and was independently recovered in large-scale analyses based on range maps rather than local detections. This convergence across complementary analytical designs supports the robustness of our results.

Trophic structure of each local assemblage (BBS route x year) was characterized as the proportional or relative species richness of ten trophic guilds: omnivores, invertivores (predators of invertebrates), vertivores (predators of vertebrates), aquatic herbivores, terrestrial herbivores, aquatic predators, granivores, frugivores, nectarivores and scavengers. Species were assigned to guild following the diet categories in the AVONET dataset (10). Robustness to alternative guild definitions and uncertainty in species-to-guild assignments was evaluated in sensitivity analyses. See the specific section for *sensitivity analyses* below.

To harmonize taxonomy across the diet and BBS datasets, we aggregated subspecies to species level, resolved synonyms using Avibase (52) and the IUCN Red List (53) (via the rredlist R package, June 2024 (54)), and excluded records with ambiguous taxonomy (e.g., unidentified taxa, hybrids, or dual-species labels). The final dataset comprised 31,251 local assemblages (i.e., unique BBS route-year combinations) from 4,226 routes sampled between 1997 and 2022, encompassing 574 species and approximately 21 million individual records.

BBS routes in North America: Ecological proxies and statistical analyses

Directly quantifying the total resource energy available to each guild, species energetic requirements, and niche partitioning across tens of thousands of assemblages spanning North America over decades is not feasible. We therefore relied on three ecological proxies. For the first proxy, trophic-dynamic ecology and metabolic theory imply that consumer biomass cannot be generated or maintained without prior resource acquisition, assimilation and energy allocation to maintenance and growth (1-3). Therefore, a higher total biomass of a guild suggests that a larger minimum amount of environmental energy was available and accessible to that guild. This interpretation does not imply a direct one-to-one relationship between the supply of environmental energy and consumer biomass, as various factors such as trophic-transfer efficiency, resource quality, food-web complexity, and top-down control can influence the extent to which available energy is ultimately reflected as consumer biomass (13, 55-60). Nevertheless, broad-scale studies of birds show that assemblage abundance, biomass and/or energy use generally increase with environmental energy availability or productivity, and analogous relationships have been reported for mammalian and terrestrial herbivore biomass across productivity gradients (12, 14, 16, 61-63). We therefore used variation in total guild biomass as a coarse proxy for the environmental energy accessible to each guild. Specifically, the total biomass for each guild g was calculated as follows:

$$B_{a,g} = \sum_{i \in g} N_{a,i} M_i \qquad \text{Eq. 1}$$

where $B_{a,g}$ is the total biomass of guild *g* in assemblage *a*, *i* denotes each species belonging to guild *g*, $N_{a,i}$ is the abundance of species *i* recorded in assemblage *a*, and M_i is the mean adult body mass of species *i*. Species abundances were obtained from the North American Breeding Bird Survey (BBS) (27), and body mass data were sourced from AVONET (10). When body mass is expressed in grams, $B_{a,g}$ represents total guild biomass in grams. Our primary conclusions remained consistent even when the proxy of total guild biomass was excluded from the analysis.

Species energetic demand was approximated as the number of individuals sustained per unit biomass calculated as:

$$D_{a,g} = \frac{A_{a,g}}{B_{a,g}} \qquad \text{Eq. 2}$$

where $D_{a,g}$ is the number of individuals sustained per unit biomass in guild *g* in assemblage *a*, $A_{a,g}$ is the total abundance of all individuals belonging to guild *g* in assemblage *a*, and $B_{a,g}$ is the total guild biomass calculated using Eq. 1. Higher values of $D_{a,g}$ indicate that more individuals are sustained per unit biomass, which is expected for guilds composed of smaller-bodied species with lower per-individual energetic requirements. A species energetic demand could also be represented by its metabolic rate, and basal metabolic rates can be approximated by allometric relationships (2, 64, 65) yielding similar results (see sensitivity analyses below). However, using the number of individuals sustained per unit biomass also allowed us to decompose two abundance-related processes and more explicitly link our results to the More Individual Hypothesis (4, 15, 17), which predicts that greater energy availability can promote species richness by sustaining larger populations and reducing extinction risk. As both proxies

are linked to total guild abundance, they can be interpreted as complementary components of the same mechanism.

Niche partitioning reflects ecological differentiation among coexisting species (21), often driven by divergence in foraging strategies in birds (23, 66). Because foraging strategies in birds are strongly linked with morphological traits (23), we interpreted greater within-guild morphological diversity as evidence of stronger differentiation in foraging-related niches and used it as a proxy for niche partitioning. For each BBS route–year and guild, we quantified variation among species (as coefficients of variation, CV) in nine foraging-related traits: beak length (culmen), beak length (nares), beak width, beak depth, tarsus length, wing length, first secondary length, tail length, and body mass (10). All traits were $\log_{10}$-transformed before calculating CVs. We then summarized the nine standardized trait-specific CVs into a single composite index of morphological diversity following Lefcheck (67). This composite was calculated as a weighted sum of the standardized CVs, with weights derived from their fixed-effect coefficients in a model including all nine traits (see details in supplementary text 9). Guilds represented by a single species were assigned a value of zero reflecting no interspecies morphological diversity.
The composite index provides one integrated measure of foraging-related morphological diversity, allowing niche partitioning to be represented by one predictor, as for resource amount and species energetic demand (Fig. 1). Models using the composite index and models including the nine trait-specific CVs separately are virtually the same (supplementary text 9) supporting that using the composite index represents only a conceptual simplification. See sensitivity analyses on alternative treatments of morphological diversity and the composite index below.

To evaluate how total guild biomass, individuals per unit biomass, and morphological diversity explain variation in relative species richness across trophic guilds within local bird assemblages, we fitted linear mixed-effects models using $\log_{10}$-transformed relative species richness as the response variable. The $\log_{10}$-transformation emphasized proportional rather than absolute differences in guild representation, reducing the leverage of highly represented guilds, and improving comparability between rare and common guilds (see sensitivity analyses below). Each observation corresponded to one trophic guild within one local bird assemblage. Fixed effects were total guild biomass, individuals per unit biomass, and morphological diversity, whereas random effects accounted for the hierarchical spatial and temporal structure of the data (see details in supplementary text 15). Fixed effects were standardized prior to modelling to facilitate coefficient comparison. Because these guild-level predictors are undefined when guild richness is zero, analyses were restricted to guilds represented by at least one species; results therefore describe variation in relative species richness conditional on guild presence. We quantified model explanatory power using the $R^2_{marginal}$ of Nakagawa and Schielzeth (68), which estimates the variance explained by the fixed effects of the model, and assessed predictor importance by variance partitioning: differences in $R^2_{marginal}$ between the full model and the same model excluding one predictor at a time. We visualized the effects of standardized predictors using partial residual plots, which show the adjusted relationship between each predictor and the response while accounting for the other predictors in the model (Fig. 2), by using the R package

visreg (69). Models were fitted with the lmer function in the lme4 package (70), $R^2_{marginal}$ was calculated with r.squaredGLMM in MuMIn (71).

BBS routes in North America: The potential effect of niche processes beyond the More Individual Hypothesis

In the main analysis, total guild biomass, individuals per unit biomass, and morphological diversity jointly explained a large proportion of the variation in relative species richness across trophic guilds, suggesting that energetic and niche processes may be partly coupled (5). However, morphological diversity also appeared to retain an independent association with guild richness. To explore the importance of this predictor further, we repeated the analysis using rarefied guild richness, thereby controlling for differences in abundance among guilds.

For each route-year, we identified the smallest number of individuals recorded among the guilds present and retained only route-years in which this minimum was at least five individuals. We then used individual-based rarefaction to estimate the expected number of species in each guild if all guilds within an assemblage had been represented by the same number of individuals. Using these rarefied values, we recalculated relative species richness and modelled it as a function of morphological diversity alone. Model performance was assessed using $R^2_{marginal}$ (68).

This analysis can also be interpreted as a sensitivity test for imperfect and uneven sampling across guilds. If some guilds are more completely sampled than others, observed richness may differ partly because more individuals were detected rather than because more species were truly present. By using individual-based rarefaction, we standardized richness estimates to the same number of detected individuals across guilds within each assemblage, thereby reducing the influence of unequal abundance, potentially due to uneven detectability, on the response variable.

BBS routes in North America: Sensitivity analyses

We assessed the robustness of our results using a broad set of 16 sensitivity analyses, all of which converged on the same qualitative inference: proxies of energetic and niche processes are strongly associated with variation in relative species richness across trophic guilds within bird assemblages. First, we repeated the analyses using an alternative dominant-resource classification and a probabilistic reassignment of species based on dietary proportions (supplementary text 1). Second, we addressed the proportional nature of the response by using compositional-data analyses and replacing relative guild richness with absolute guild richness as dependent variable (supplementary text 2). Third, we controlled for under sampling using as a dependent variable the Chao1-corrected richness estimate (supplementary text 7). Fourth, we tested a key prediction of the More Individuals Hypothesis and our total guild biomass mechanisms: abundance of a target species is positively related to its guild biomass, after excluding the biomass of the target species (supplementary text 5). Fifth, we used two alternative abundance-independent proxies for species energetic demand estimating basal metabolic rates from allometric relationships (supplementary text 3). Sixth, we used three alternative measurements of diversity in foraging strategies, our proxy for niche partitioning, by

standardizing species richness across guilds within routes before estimating morphological variation, excluding single-species guilds, replacing the coefficient-of-variation-based composite variable with one defined by mean pairwise trait distances (supplementary text 4). We also tested all nine trait-specific CV as predictors instead of the composite index (supplementary text 9). Seventh, we estimated response and explanatory variables from different halves of each BBS survey to reduce potential mathematical coupling (each survey encompasses 50 stops; supplementary text 6). Eighth, we re-evaluated model fit ($R^2_{marginal}$) via cross-validation analyses (supplementary text 8). Finally, we assessed the potential spatial and temporal autocorrelation of data (supplementary text 10). Taken together, the consistency of the results across a broad set of sensitivity analyses using alternative guild definitions, predictors, response variables, sampling corrections, and statistical approaches supports our central ecological inference that energetic and niche processes are strongly associated with variation in the relative species richness of trophic guilds within bird assemblages.

Large-scale assemblages worldwide: Defining bird assemblages and their trophic structure

To assess the relationship between the relative species richness among guilds and energetic and niche processes in large-scale bird assemblages, we defined large-scale assemblages by overlaying global bird distribution maps (29) onto 10,753 equal-area grid cells (25, 30). We considered species co-occurring in the same grid cell as large-scale bird assemblages (25, 30). We obtained species distributions of birds from BirdLife International (29) (www.birdlife.org; accessed in November 2021), retaining only polygons classified as extant or probably extant, and used native and reintroduced areas to define species' ranges (25, 30). We then projected the species distributions onto a regular grid, with a resolution of ~110 km x 110 km (25, 30). We limited the analyses to 8,648 species occurring in grid cells with ≥ 50% of their area classified as land (30) and with available information on their diets. In each large-scale assemblage, we quantified the relative species richness of each trophic guild. Species were classified into one of ten guilds based on the AVONET database (10): omnivores, invertivores, granivores, frugivores, nectarivores, scavengers, aquatic predators, terrestrial herbivores, aquatic herbivores, and vertebrate predators.

Large-scale assemblages worldwide: Ecological proxies and statistical analyses

We used the same three ecological predictors as in the local-scale analyses. Morphological diversity was calculated using the same approach as in the local analyses but applied to the set of species co-occurring in each grid cell. In contrast, because abundance data are not available for all species and regions of the world, total guild biomass and the number of individuals per unit biomass were calculated from global species-level estimates of population density provided by Santini et al. (31). Since these density estimates were applied to grid cells of fixed area (~110 × 110 km), they provide coarse estimates of species abundance per grid cell. To account for the fact that each grid cell may contain multiple habitats differing in their suitability for each species, we first calculated the proportional cover of each habitat within each grid cell using the global habitat raster maps of Jung et al. (72). We then combined these habitat proportions with IUCN species-level habitat-suitability information to weight our abundance

686 estimates by the amount of suitable habitat available to each species in each grid cell. Finally,
687 we calculated total guild biomass and individuals per unit biomass using equations 1 and 2.
688 These global density estimates represent global species average densities rather than spatially
689 explicit estimates of local abundance. They therefore do not capture the distinct spatial variation
690 in density/abundance within species ranges across species, attenuating any real association and
691 increasing the probability to detect false-negative associations between our hypothetical
692 ecological processes and the relative richness of trophic guilds across grid cells. Thus, any
693 association between these average estimates and relative species richness among guilds should
694 be conservative.
695
696 Santini et al. (31) provided broad species-level predictions for 8,047 of the 8,648 species
697 retained in our global assemblage dataset. The remaining 601 species were assigned density
698 estimates using a hierarchical imputation procedure based on body mass and taxonomy (see
699 supplementary text 16 for details on uncertainty and imputation).
700
701 Sensitivity analyses showed that inferences were similar when considering uncertainty in
702 density estimates provided by Santini et al. (31) (supplementary text 11), when morphological
703 diversity was quantified as the mean pairwise distance among species in an nine-trait
704 morphological space rather than with the composite variable (supplementary text 12), when
705 species energetic demand was quantified using the median basal metabolic rate of species
706 within guilds (supplementary text 13), and when assemblages were redefined at the finer
707 spatial grain of grid cell × habitat combinations rather than whole grid cells (supplementary text
708 14).
709
710 **Global similarity in the trophic structure**
711 To assess global similarity in trophic structure, we estimated how well a single global (average)
712 pattern of guild proportions describes the trophic structures in all grid cell assemblages. We
713 fitted a linear mixed-effects model in which each observation corresponded to a trophic guild
714 within a grid cell, with the response variable being the proportion of species in that guild (relative
715 guild richness) and trophic guild category (ten levels) as a fixed effect predictor. Grid-cell identity
716 was included as a random intercept effect. We quantified global similarity using the $R^2_{marginal}$
717 provided by Nakagawa & Schielzeth (68), which measures the fraction of variation in guild
718 proportions explained by the global average pattern of each guild. High $R^2_{marginal}$ values indicate
719 that a single global average captures most of the variation in grid-cell proportions. We interpret
720 a high similarity in trophic structure among bird assemblages that differ in species composition,
721 richness and underlying historical, environmental, ecological and evolutionary processes as
722 evidence for global convergence.
723
724 Sensitivity analyses showed that the global signal was robust to alternative representations of
725 trophic structure. Specifically, we obtained the same qualitative result when species were
726 reassigned to trophic guilds according to their dominant dietary resource (obtained from
727 EltonTraits) (9), and also when assemblages were represented as continuous diet profiles based

on the average proportional use of different resources by the species present, rather than as proportions of species assigned to discrete guilds (supplementary text 12).

Global vs regional trophic structures

The existence of global similarities does not preclude possible regional variations. To identify regional spatial patterns in the trophic structure of bird assemblages worldwide, we searched for dissimilarities in guild proportions across grid cells worldwide (36-38). We computed Euclidean distances between all pairs of assemblages based on their guild proportions and performed hierarchical clustering using Ward's method (73). The optimal number of clusters was determined using the silhouette index (74) via the *NbClust* package in R (75), resulting in three geographically coherent groups corresponding to tropical, non-tropical, and extreme climatic regions.

To assess how well the global model captured patterns of trophic structure within each region, we compared the observed and predicted values of guild proportions across tropical, non-tropical, and extreme environments. To quantify the relative importance of regional differences versus global similarities, we compared two models describing variation in guild proportions across grid cells. The "global" model included trophic guild as the only fixed effect, implying a common trophic structure across all regions. The "regional" model additionally included a guild × region interaction, allowing mean guild proportions to differ among the three regions. If regional differences in trophic structure are strong, the regional model should yield a markedly better fit; if it provides only modest improvement, regional patterns can be viewed as statistically detectable, and ecologically relevant, but arguably minor deviations from an overarching global pattern. Model fit was quantified using the $R^2_{marginal}$ (68).

Human footprint

We assessed whether grid-cell deviations from the trophic structure predicted by the finer-grained regional model were associated with the Human Footprint values. We used the regional model described above. For each grid cell and guild, we calculated a residual as the observed minus the fitted guild proportion. We then summarized the overall deviation of each grid cell as the root mean squared deviation across guilds, calculated as the square root of the mean squared residuals of all guilds in that cell. Thus, root mean squared deviation provides one value per grid cell, measuring how strongly the trophic profile of each assemblage departs from its expected regional profile. To quantify Human Footprint, we overlaid each grid cell on the 2019 Human Footprint raster (76) and extracted the area-weighted mean value of the intersecting pixels. This value was z-standardized, by subtracting the mean and dividing by the standard deviation, and was then used to test whether grid cells with higher mean Human Footprint deviated more or less from their expected regional trophic profile.

SUPPLEMENTARY TEXT

supplementary text 1: Species' assignment to guilds based on dietary information from the EltonTraits dataset

We tested whether our results depended on the trophic guild classification used in the main analyses by reclassifying species using EltonTraits dietary data, which report the estimated fraction of each species' diet, in 10% intervals, assigned to eight resource categories: invertebrates, vertebrates, fruits, seeds, nectar, carrion, aquatic prey, and other plant material (9). We were unable to harmonize species information for 12 species between the Breeding Bird Survey and EltonTraits datasets and therefore excluded all route-year assemblages in which those species occurred. In total, the two sensitivity analyses on alternative guild classification included 31,048 bird assemblages.

In a first sensitivity analysis, species were classified as trophic specialists when a single resource category represented 60% or more of the diet; all remaining species were classified as omnivores. We then recalculated relative species richness of the nine guilds (one per resource category plus omnivores) for each North American bird assemblage and followed the same mixed-effects modelling framework used in the main text. Model performance closely matched that of the primary analyses ($R^2_{marginal}$ = 0.895). Total guild biomass (estimate ± s.e. = 0.167 ± 0.001), individuals per unit biomass (0.136 ± 0.001), and morphological diversity (0.417 ± 0.001) all remained positively associated with relative guild richness (all $p < 0.001$). Morphological diversity retained the largest unique contribution to model fit ($\Delta R^2_{marginal}$ = 0.180), whereas total guild biomass and individuals per unit biomass contributed $\Delta R^2_{marginal}$ = 0.012 and 0.011, respectively.

In a second sensitivity analysis, we evaluated whether the results were robust to uncertainty in assigning species with mixed diets to a single trophic category. To do so, we ran 100 null-model iterations in which each species was reassigned to one of the eight EltonTraits resource categories with probabilities proportional to its reported dietary composition. Consequently, there were no omnivores in this second sensitivity analysis. For each iteration, we recalculated both response and predictor variables and refitted the same mixed-effects models used in the main analysis. Results were qualitatively unchanged. Across all 100 null-model iterations, total guild biomass, individuals per unit biomass, and morphological diversity remained positively associated with the relative species richness of guilds within assemblages (mean standardized estimates = 0.293, 0.248, and 0.209, respectively; mean s.e. = 0.00077, 0.00071, and 0.00067; $p < 0.001$ in all 100 iterations). Model fit remained substantial (mean ± s.d. $R^2_{marginal}$ = 0.77 ± 0.03). On average, the unique contributions of total guild biomass, individuals per unit biomass, and morphological diversity were $\Delta R^2_{marginal}$ = 0.10, 0.09, and 0.08, respectively, with 0.49 of marginal R^2 shared among predictors.

Together, these two sensitivity analyses show that our ecological inference is robust to alternative trophic classifications and to uncertainty in the assignment of guilds to species exploiting multiple resource types.

supplementary text 2: Compositional data analyses and absolute species richness

To verify that our inferences are not driven by the unit-sum constraint of proportional data, we performed two sensitivity analyses using: (i) compositional data analyses (77), (ii) analyses predicting the total species richness per guild instead of the relative species richness.

i) Compositional analyses

The relative contribution of trophic guilds within a community is inherently compositional: guild proportions are strictly positive and constrained to sum to one. In such closed systems, analyzing raw proportions can be misleading, because an apparent increase in one guild must necessarily be offset by decreases in one or more others, generating covariation. To avoid these artefacts, compositional data can be analyzed using log-ratio transformations that respect their constrained geometry.

We analyzed guild composition using an additive log-ratio (ALR) approach. For each survey, we selected *invertivores* as the fixed reference guild, as this guild was present in nearly all surveys and therefore maximized data retention and comparability. For every other guild *g* in assemblage *a*, we defined the response variable as $\mathrm{ALR}_{\mathbf{a},\mathrm{g}} = \log\left(\frac{\mathbf{p}_{\mathbf{a},\mathbf{g}}}{\mathbf{p}_{\mathbf{a},\mathrm{ref}}}\right)$, where $\mathbf{p}_{\mathbf{a},\mathbf{g}}$ is the proportion of species richness belonging to guild *g* in assemblage *a*, and $\mathbf{p}_{\mathbf{a},\mathrm{ref}}$ is the proportion of invertivores in the same assemblage *a*. This transformation shifts the analysis from modelling a closed multivariate composition to modelling relative deviations from a common ecological baseline, namely how much more or less represented each guild is relative to invertivores. Surveys in which a given guild was absent were excluded for that guild to ensure that all log-ratios were well defined.

To keep predictors on the same relative scale as the response, all explanatory variables were expressed contrasts in assemblage *a* relative to the reference guild. For each guild *g* in each assemblage *a*, we computed differences in total biomass, individuals per unit biomass, and morphological diversity as $\boldsymbol{\Delta X_{a,g} = X_{a,g} - X}_{\mathrm{ref}}$, where $\boldsymbol{X_{a,g}}$ is the value of a given predictor for guild *g* in assemblage *a*, and $\boldsymbol{X}_{\mathrm{ref}}$ is the corresponding value for invertivores in the same assemblage *a*. These contrasts remove survey-level differences in absolute magnitude and focus inference on within-community structure.

We fitted the ALR model using a simpler random-effects structure than in the main BBS model. The main model allowed baseline guild richness to vary across the full spatial and temporal hierarchy of the data, whereas the ALR model retained random intercepts for local bird assemblages, defined as each BBS route–year, and for states. This simplification was used because the full hierarchy was too complex for the ALR model: some random-effect levels explained almost no additional variation and generated convergence warnings. The simpler model was therefore more stable while retaining the main sources of non-independence in the data.

To interpret model predictions on the original compositional scale, we reconstructed guild proportions from predicted ALR values. Predicted log-ratios for non-reference guilds were modified to obtain ratios as follows $\boldsymbol{r_g = \exp\left(\widehat{\mathrm{ALR}_g}\right)}$. The reference guild was assigned $\boldsymbol{r_{\mathrm{ref}} = 1}$ by definition. Within each survey, these ratios were then normalised to sum one as follows $\boldsymbol{\widehat{p_g} = \frac{r_g}{\sum_j r_j}}$, yielding predicted proportions that are strictly positive, sum to one, and remain consistent with the geometry of compositional data.

Model performance was evaluated using two complementary measures. First, we computed a clr-space (Aitchison) pseudo-R^2 by comparing observed and predicted compositions after clr transformation, quantified as $(1 - SSE/SST)$ in clr space. These metric measures agreement in log-ratios, rather than in raw proportions, and can therefore take very high values when the dominant relative gradients in composition are strongly structured. Second, to provide a more intuitive summary of predictive accuracy at the community level, we calculated the median survey-level Pearson R^2, defined as the median across surveys of the squared correlation between observed and reconstructed guild proportions within each survey. This statistic reflects the typical concordance between observed and predicted compositions for a community.

Using invertivores as the reference guild, the clr-space pseudo-R^2 was 0.99, while the median survey-level R^2 was approximately 0.964, indicating high agreement for a typical community. The three predictor contrasts remained strongly positive (total guild biomass: estimate ± s.e. = 0.533 ± 0.002; individuals per unit biomass: 0.403 ± 0.002; morphological diversity: 0.653 ± 0.002; all $p < 0.001$). To test whether these values depended on the choice of ALR denominator, we repeated the full analysis using alternative reference guilds whenever data coverage allowed. Median survey-level R^2 values were similar across feasible choices (Granivore: 0.91; Aquatic predator: 0.87; Vertivore: 0.88; Frugivore: 0.88; Scavenger: 0.88). Some guilds (aquatic herbivores, terrestrial herbivores, nectarivores) could not be used as reference categories because they were absent from a large fraction of surveys, leading to insufficient data after filtering.

To assess whether the high goodness-of-fit (clr-space pseudo-R^2) could arise from in-sample evaluation, we performed leave-group-out cross-validation, withholding entire states or survey routes from model fitting and predicting guild compositions for these unseen units. Under this stringent out-of-sample validation, predictive performance remained high, with median survey-level R^2 values around 0.96 and clr-space pseudo- R^2 values remaining close to 0.99. This demonstrates that the high agreement reflects a stable and reproducible structure in relative guild composition across space.

Taken together, these analyses show that the compositional patterns captured by the model are robust to the choice of reference guild and generalize well beyond the data used for fitting. The very high fit values in log-ratio space should not be interpreted as perfect prediction, but rather as evidence that most of the relative differences among trophic guilds within communities follow a consistent and predictable structure. The strong concordance observed under strict out-of-

sample validation supports the interpretation that the compositional framework captures genuine ecological regularities in guild proportionality.

In the main text we report a standard mixed-effects analysis because it is easier to interpret and communicate (effects are expressed directly on a single response scale and are familiar to most readers). The compositional ALR analysis presented here is a complementary robustness check that treats guild proportions in a formally correct way for closed data. Both approaches support the same ecological message: the main predictor blocks capture consistent structure in guild proportionality across communities.

ii) Total species richness as explanatory variable

We also repeated the main analysis using absolute guild species richness instead of relative guild richness as the response variable. Specifically, we fitted a linear mixed-effects model with log-transformed species richness per guild as the response and the same three standardized ecological proxies used in the main model: total guild biomass, individuals per unit biomass and morphological diversity. Ecological inferences were similar to those in the main analyses. The three predictors explained most of the variance ($R^2_{marginal}$=0.89) and showed strong positive associations with guild richness (estimate ± s.e. for total guild biomass = 0.528 ± 0.002, individuals per unit biomass = 0.447 ± 0.002; and morphological diversity = 0.762±0.002 ; all $p < 0.001$).

Together, the main analysis and these two sensitivity analyses show that our conclusions are robust to methodological choices in the analytical framework.

supplementary text 3: Alternative body-mass-based proxies for species energetic demand

We performed two sensitivity analyses to test whether our conclusions were robust to alternative estimates of species energetic demand. Instead of using individuals per unit biomass, as in the main text, we used estimates of basal metabolic rate (BMR) derived from a general allometric relationship supported for birds (64, 65): $BMR_i = M_i^{2/3}$ where BMR_i is the body-mass-based metabolic proxy of species *i*, and M_i is the average adult body mass of species *i*. We then aggregated species-level values to calculate guild-level metabolic proxies for each guild *g* in each assemblage *a*, using three approaches. First, we calculated the mean BMR of all species present in guild g and assemblage (a), representing the typical metabolic demand of species in that guild: $\frac{1}{S_{a,g}} \sum_{i \in g} M_i^{2/3}$, where $S_{a,g}$ is the number of species in guild (g) within assemblage (a). Second, we calculated the abundance-weighted mean BMR, representing the typical metabolic demand of the average individual in guild (g) and assemblage (a): $\frac{\sum_{i \in g} N_{a,i} M_i^{2/3}}{A_{a,g}}$ where $N_{a,i}$ is the abundance of species *i* in assemblage *a*, and $Aa, g = \sum_{i \in g} N_{a,i}$ is the total abundance of guild *g* in assemblage *a*. The two guild-level BMR proxies were log-transformed and standardized before modelling. We then replaced individuals per unit biomass in the main model with each of these alternative proxies while retaining total guild biomass and morphological diversity as the other two predictors. Model performance was similar across the two alternative guild-level BMR proxies: $R^2_{marginal}$ when using the mean BMR = 0.868, and using abundance-weighted mean BMR = 0.869. In all cases, the results supported the same ecological interpretation as the main analysis (estimate ± s.e. for morphological diversity was 0.340 ± 0.001 when using the mean BMR, and 0.334 ± 0.001 when using abundance-weighted mean BMR, whereas for individuals per unit biomass was -0.185 ± 0.001 and -0.189 ± 0.001, respectively; all $p < 0.001$). These sensitivity analyses therefore show that our inferences are robust to alternative body-mass-based estimates of species energetic demand.

supplementary text 4: Sensitivity analyses for morphological diversity

To support the robustness of our ecological inferences regarding the role of niche processes, we conducted three sensitivity analyses focused on our proxy for morphological diversity: (i) calculating the coefficient of variation (CV) of traits after standardizing the number of species across guilds; (ii) excluding guilds represented by only one species and bird assemblages containing guilds represented by only one species, for which the coefficient of variation was zero; and (iii) measuring morphological diversity as the mean pairwise distance among species.

<u>i) Calculating the coefficient of variation (CV) of traits after standardizing the number of species across guilds</u>

Morphological variation within a trophic guild can be influenced by the number of species used to calculate it. To test whether our results were affected by this issue, we repeated the analyses after recalculating morphological variation while holding species richness constant across guilds within each BBS route.

We began with the dataset used in the main analyses, in which each bird assemblage was defined by the relative species richness of each guild for each combination of Breeding Bird Survey route and year. For each assemblage, we identified the smallest number of species recorded among its guilds, considering only guilds with at least two species so that variation could be estimated. This value was used as the target richness for that bird assemblage. Within each guild in that bird assemblage, we randomly sampled that number of species without replacement to obtain rarefied species assemblages. In this way, all guilds with at least two species within a given bird assemblage contributed the same number of species to the calculation of morphological variation; guilds represented by fewer than two species retained CV = 0, as in the main analysis.

Using each rarefied species assemblages, we recalculated the coefficient of variation for the same nine traits used in the main analysis. These trait-specific coefficients of variation were then combined into the same composite variable of morphological diversity described for the main models. We then refitted the main mixed-effects model relating guild relative richness to guild biomass, individuals per unit biomass, and the composite variable of morphological diversity, keeping the same hierarchical random-effects structure as in the main analysis.

Because random subsampling introduces stochastic variation, we repeated the full procedure 100 times. In each iteration, we (1) equalized species richness across guilds within each route-year assemblage by random subsampling, (2) recalculated the coefficients of variation for the nine morphological traits, (3) rebuilt the composite variable, and (4) refitted the main model with the three predictors (total guild biomass, individuals per unit biomass, and morphological diversity). Robustness was assessed from the marginal R^2 of the final mixed-effects model, which was highly stable across the 100 rarefaction-based repetitions (mean = 0.7948, s.d. = 0.00041, s.e. = 0.00004). We then quantified the unique contribution of each predictor as the reduction in $R^2_{marginal}$ when that predictor was removed from the full model while the other predictors were retained. Under this definition, total guild biomass showed the largest mean

unique contribution, followed by individuals per unit biomass and morphological diversity (non-shared $R^2_{marginal}$=0.17, 0.16, 0.05, respectively). Nevertheless, as in the main model, most of the explained variance was not attributable to a single predictor (shared $R^2_{marginal}$ = 0.42). Fixed-effect estimates were also highly stable across repetitions: mean estimates were 0.40 for total guild biomass, 0.34 for individuals per unit biomass, and 0.16 for morphological diversity, with very small between-iteration variation (standard deviation = 0.00053, 0.00048, and 0.00059, respectively). Model-based standard errors were likewise nearly constant across repetitions (mean s.e. = 0.00082, 0.00075, and 0.00074, respectively).

Notably, the relative contribution of morphological diversity became stronger in more information-rich subsets, where trait dispersion was estimated from guilds represented by larger numbers of species. For example, when analyses were restricted to guilds with at least four species and to route-year assemblages retaining at least three such guilds, the unique contribution of morphological diversity increased to 0.1179. This pattern is consistent with the expectation that within-guild morphological variation is estimated more precisely when based on richer species samples. Importantly, however, the qualitative conclusion was unchanged across all sensitivity analyses: total guild biomass, individuals per unit biomass, and morphological diversity each contributed to explaining variation in relative species richness among guilds within bird assemblages.

ii) Excluding guilds with only one species and coefficient of variation equal to zero

In the main analysis, we set morphological diversity (coefficient of variation) to 0 when a trophic guild was represented by a single species (S = 1), reflecting no interspecific variance in morphological diversity. To ensure that this decision did not affect our inferences, we repeated the same mixed-effects model under two progressively stricter data filters: (i) removing only the affected guild observations ("drop S=1 rows"; 124,818 observations across 31,251 bird assemblages and (ii) removing entire route-year assemblages whenever any guild had S = 1 ("drop S=1 routes"; 10,530 observations across 2,297 bird assemblages). Each observation is the relative species richness of one guild in a bird assemblage (BBS route x year). In all models, we retained the same three predictors: total guild biomass; individuals per unit biomass, and a composite variable derived from morphological diversity. Our results showed that the qualitative inference was unchanged: the three variables remained positively associated with relative species richness of guilds (p-value < 0.001 for all variables; table S1).

Model	Total guild biomass	Individuals per unit biomass	Morphological diversity (composite)	$R^2_{marginal}$
Drop guild obs.	0.187 ± 0.001	0.223 ± 0.001	0.145 ± 0.001	0.751
Drop assemblage	0.177 ± 0.001	0.198 ± 0.001	0.148 ± 0.001	0.689

Table S1. Robustness of inferences to excluding single-species guilds. Values are standardized coefficient estimates ± standard errors from linear mixed-effects models. "Drop guild obs." excludes guild-level observations in which a trophic guild was represented by a single species, whereas "Drop assemblage" excludes entire Breeding Bird Survey route-year

assemblages whenever any guild within the assemblage was represented by a single species. All predictors remained positive and statistically significant in both models ($P < 0.001$).

iii) Measuring morphological diversity as the mean pairwise distance among species

As an alternative to the coefficient-of-variation-based composite used in the main analysis, we quantified morphological diversity within each trophic guild using mean pairwise distance (MPD). MPD was calculated from Euclidean distances among species in a nine-dimensional morphological trait space defined by the same nine traits used in the main analysis. All nine traits were $\log_{10}$-transformed and standardized to mean 0 and standard deviation 1 before calculating pairwise distances.

We first constructed a species × species Euclidean distance matrix using this standardized morphological trait space. MPD was then calculated separately for each trophic guild within each local bird assemblage, defined as each survey × trophic guild combination. For each guild within each assemblage, MPD was computed as the mean of all pairwise morphological distances among the species present. Guilds represented by a single species were assigned MPD = 0 because no within-guild species pairs were available.

We then fitted the same mixed-effects model structure used in the main analysis but replaced the CV-based morphological diversity composite with the MPD-based metric. We also fitted reduced models in which each predictor was removed in turn to evaluate how model coefficients and $R^2_{marginal}$ changed when total guild biomass, individuals per unit biomass, or MPD-based morphological diversity were excluded. The results were qualitatively consistent with the main analysis, indicating that the positive association between morphological diversity and relative guild species richness was not dependent on the specific morphological diversity metric used (table S2). However, the relative importance of the predictors differed, with MPD-based morphological diversity showing the smallest unique contribution to $R^2_{marginal}$ ($\Delta R^2_{marginal} = 0.041$), compared with total guild biomass ($\Delta R^2_{marginal} = 0.183$) and individuals per unit biomass ($\Delta R^2_{marginal} = 0.206$).

Model	Total guild biomass (estimate ± s.e.)	Individuals per unit biomass (estimate ± s.e.)	Morphological diversity (MPD) (estimate ± s.e.)	$R^2_{marginal}$
Full model	0.405 ± 0.001	0.364 ± 0.001	0.152 ± 0.001	0.79
Without total guild biomass	NA	0.134 ± 0.001	0.397 ± 0.001	0.60
Without indiv. per unit biomass	0.122 ± 0.001	NA	0.361 ± 0.001	0.58
Without MPD	0.523 ± 0.001	0.447 ± 0.001	NA	0.75

Table S2. Robustness of inferences using an alternative proxy for morphological diversity. Values are standardized coefficient estimates ± standard errors from linear mixed-effects models. Morphological diversity was quantified as the mean pairwise distance (MPD) among

species within each trophic guild and local bird assemblage, using Euclidean distances calculated from the same nine morphological traits used in the main analysis. The full model included total guild biomass, individuals per unit biomass, and MPD-based morphological diversity as fixed effects, with the same random-effects structure as in the main analysis. "Without" rows correspond to reduced models refitted after removing the indicated predictor. "NA" indicates that the predictor was not included in that model. $R^2_{marginal}$ represents the variance explained by the fixed effects.

supplementary text 5: Assessing the relationship between species abundance and guild biomass

In the main text, we asked whether guilds associated with more resources also support more individuals, as expected under the more-individuals hypothesis. Because resource biomass cannot be measured directly across the full Breeding Bird Survey, we used total guild biomass as an indirect proxy for the resource or energy pool available to each trophic guild. Here, we tested a direct expectation of this interpretation: if total guild biomass captures variation in guild-level resource availability, then focal species should tend to be more abundant where the rest of their guild also has greater biomass.

To test this expectation while avoiding direct circularity, we carried out a species-level leave-one-out analysis. For each focal species in each Breeding Bird Survey route × year and trophic guild, we recalculated guild biomass after excluding the biomass contributed by that focal species. We then modelled focal species abundance as a function of this leave-one-out guild biomass. This model used a negative binomial error distribution to account for overdispersed count data and included species and route-year fixed effects. These fixed effects were used to compare changes within species while controlling for conditions shared by all observations from the same route-year, rather than to interpret species- or route-specific coefficients. In other words, the analysis tested whether a given species tended to be more abundant in route-years where the rest of its guild had greater biomass.

We also tested whether this relationship differed between rare and common species. To do this, we classified species into four rarity classes according to their occupancy across route-years, that is, according to the number of route-years in which each species was recorded. Species in the lowest occupancy quartile were treated as the rarest, whereas species in the highest quartile were treated as the most common. We then allowed the relationship between abundance and leave-one-out guild biomass to vary across these four rarity classes.

The relationship was positive in all four rarity classes. Species tended to be more abundant in route-years where the rest of their guild had greater biomass, even though the focal species itself had been removed from the biomass predictor. Statistical support was strongest outside the rarest occupancy quartile: the relationship was significantly positive in three of the four rarity classes, whereas the rarest species showed a positive but non-significant association (table S3).

Although this analysis does not demonstrate causation, it supports the expectation that species tend to reach higher abundances in guild contexts with greater biomass. It also shows that the biomass–abundance relationship is not solely a mechanical consequence of species contributing to their own guild biomass. Thus, the leave-one-out analysis is consistent with the more-individuals interpretation and supports the use of total guild biomass as an ecological proxy for guild-level resource availability.

Rarity class	Estimate	SE	z	*P*
Q1 rarest	0.104	0.079	1.31	0.190
Q2	0.135	0.028	4.88	<0.001
Q3	0.090	0.025	3.60	<0.001
Q4 commonest	0.123	0.047	2.60	<0.01

Table S3. Species abundance is positively associated with guild biomass. Estimates show the relationship between focal-species abundance and log-transformed leave-one-out guild biomass, calculated after excluding the biomass contribution of the focal species from total guild biomass within each route-year × trophic guild assemblage. Species were classified into four rarity classes according to their occupancy across route-years, from the rarest species (Q1) to the most common species (Q4). Estimates are negative-binomial slopes on the log scale; positive values indicate that species tend to be more abundant in route-years where the rest of their trophic guild has greater biomass.

supplementary text 6: Estimating response and explanatory variables from different datasets

In the main text, we modelled the relative species richness of trophic guilds as a function of total guild biomass, individuals per unit biomass, and morphological diversity. However, some of the association among these variables could arise from shared statistical structure rather than from a purely ecological relationship. Species richness is often positively related to functional or morphological diversity (78, 79) and also to the number of individuals represented in an assemblage or sample (17, 80), while abundance is itself used in the calculation of total guild biomass. Consequently, part of the variance explained by the model could reflect mathematical coupling among variables. Although the analysis based on rarefied relative richness showed that the signal is not driven solely by differences in abundance, we conducted an additional sensitivity analysis to further separate the response from the explanatory variables strengthening out inference.

To do so, we took advantage of the structure of the Breeding Bird Survey. Each BBS route is approximately 39 km long and comprises 50 fixed stops separated by about 0.8 km. For each route-year, we divided the BBS route into two non-overlapping subsets of stops. We estimated the relative species richness of each trophic guild using only stops 1–25, and calculated the three explanatory variables using only stops 26–50: total guild biomass, individuals per unit biomass, and morphological diversity represented by a composite variable derived from variation in nine morphological traits within each guild. When a guild was not recorded in stops 1–25, but was represented in stops 26-50, its relative richness was recorded as 10^{-6} rather than 0 to allow the $\log_{10}$ transformation of the response. We then refitted the same mixed-effects model used in the main text.

The results remained consistent with the main ecological interpretation. The model largely explained variation in the relative species richness of guilds within assemblages ($R^2_{marginal} = 0.49$). The three predictors remained positively associated with guild relative richness (total guild biomass: estimate ± s.e. = 0.915 ± 0.007, individuals per unit biomass = 1.002 ± 0.0049, morphological diversity = 0.645 ± 0.006; all $p < 0.001$). Thus, even when guild richness and explanatory variables were estimated from different halves of the same route where conditions could differ, guilds with greater biomass, higher numbers of individuals per unit biomass, and greater morphological diversity still tended to be associated with more speciose guilds in bird assemblages.

supplementary text 7: Controlling for undersampling using Chao1 richness estimates

Observed species richness can underestimate true richness when some species are rare and therefore less likely to be detected. This issue is particularly relevant when comparing trophic guilds within assemblages, because guilds represented by many common species may appear richer than guilds containing more undetected rare species. To test whether our main results were sensitive to this form of undersampling, we performed an additional sensitivity analysis using abundance-based Chao1 richness estimates.

We used the same North American bird assemblages as in the main analyses, defined as each Breeding Bird Survey route × year combination. For each trophic guild within each assemblage, we compiled the vector of species abundances and estimated asymptotic richness using the Chao1 estimator, which corrects observed richness on the basis of the number of rare species represented by one or two individuals. Because this is an abundance-based correction, Chao1 is appropriate for our route-level data. To avoid unstable estimates in extremely sparse guild samples, we retained only route-years in which the minimum abundance recorded across guilds was at least five individuals. We then recalculated guild relative species richness by dividing the Chao1 estimate of each guild by the sum of Chao1 estimates across guilds within the same route-year.

Using these Chao1-based relative richness values as the response, we refitted the same mixed-effects modelling framework used in the main text, including the same three predictors: total guild biomass, individuals per unit biomass, and the composite variable of morphological diversity. We also retained the same hierarchical random-effects structure as in the main analyses.

Results remained strongly consistent with the main ecological interpretation. The full model largely explained variation in relative species richness of guilds within assemblages ($R^2_{marginal}$ = 0.76). All three predictors remained positively associated with Chao1-corrected relative richness (estimate ± s.e. of total guild biomass = 0.182 ± 0.003, individuals per unit biomass = 0.172 ± 0.003, morphological diversity = 0.305 ± 0.003; all $p < 0.001$). Variance partitioning further showed that morphological diversity retained the strongest independent contribution to model fitness. Removing the composite variable caused the largest decline in explanatory power ($\Delta R^2_{marginal}$ = 0.195), whereas removing total guild biomass or individuals per unit biomass produced much smaller reductions ($\Delta R^2_{margina}$ = 0.033 and 0.030, respectively). Together, these results show that our main conclusions are robust to under sampling rare species.

supplementary text 8: Cross-validated predictive performance of the mixed-effects model

The mixed-effects model used in the main analysis largely explained variation in relative species richness of guilds within assemblages ($R^2_{marginal}$=0.87). We assessed that model performance is high even when using distinct training and test data by using cross-validation. In our dataset, BBS routes can be repeated across years, and routes are grouped within states and countries. This means that training and test data can remain closely related if observations are split at random.

To address this issue, we used conservative blocked cross-validation designed for structured ecological data (81). Rather than randomly splitting individual observations, we held out entire states (within country) at a time. This is a much stricter test because it asks whether relationships estimated in one set of regions can successfully predict patterns in other regions that were not used to fit the model.

We defined five folds based on country-by-state combinations, so that all observations from a given state were assigned to the same fold. In each round, we refitted exactly the same linear mixed-effects model used in the main analysis to four folds and evaluated predictions on the held-out fold. Predictions for held-out states were based on fixed effects only, because random effects for routes or states absent from the training data cannot be estimated. This makes the test relevant to the question of whether the main ecological relationships generalize geographically.

Predictive performance remained high across all five folds. Mean ± s.d. of $R^2_{marginal}$ in training data = 0.869 ± 0.004, of $R^2_{marginal}$ in out-of-sample = 0.876 ± 0.010, and mean ± s.d. in out-of-sample RMSE = 0.198 ± 0.006. Mean fixed-effect estimates across training folds were 0.219 ± 0.001 for total guild biomass, 0.187 ± 0.001 for individuals per unit biomass, and 0.341 ± 0.001 for morphological diversity (all $p < 0.001$). Each test fold contained between 29,104 and 49,964 observations. The same relationships remained highly predictive when tested on entire states excluded from model fitting, indicating that the main results generalize robustly across geographic regions and that the high model performance is not merely a consequence of in-sample evaluation.

supplementary text 9: Composite variable

To quantify the degree of ecological differentiation within trophic guilds, we measured the diversity of morphological traits related to distinct foraging strategies. Previous literature has shown that nine morphological traits predicted well the foraging strategies of birds: culmen and nares beak length, beak width, beak depth, tarsus length, wing length, first secondary length, tail length and body mass (10, 23). We therefore decided to calculate the diversity of morphological traits as the coefficient of variation of these traits. Rather than analysing each trait separately, we summarized their joint contribution into a single composite variable representing within-guild morphological diversity (67, 82).

Our use of a composite variable was motivated by parsimony and interpretability. The aim was not to estimate the isolated effect of each morphological trait, but to capture the overall degree of morphological differentiation within each guild. This also allowed us to represent the three ecological proxies in the analysis (total guild biomass, individuals per unit biomass, and morphological diversity) with one variable each. Importantly, sensitivity analyses using the nine traits as predictors instead of the composite variable yielded the same conclusions (see below).

We constructed the composite in three steps. First, for each assemblage × trophic-guild combination, we calculated the coefficient of variation of each morphological trait across the species belonging to that guild. Here, assemblage refers to the sampling unit used in each analysis: route-year assemblages in the local BBS analyses, grid-cell assemblages in the global analyses, and cell × habitat assemblages in the habitat-based sensitivity analyses. Trait values were log10-transformed before calculating coefficients of variation. Guilds represented by fewer than two species were assigned a coefficient of variation of zero because among-species morphological variation could not be estimated. This step produced one trait-specific coefficient of variation for each assemblage × guild combination.

Second, we standardized all trait-specific coefficients of variation and fitted a linear mixed-effects model with log10-transformed relative guild richness as the response variable and the trait-specific coefficients of variation as fixed effects. The random-effects structure matched the corresponding analysis, using the relevant assemblage identifier as the grouping factor. The estimated fixed-effect coefficients from this model were then used as empirical weights for the composite.

Third, we calculated the composite variable as the weighted sum of the standardized trait-specific coefficients of variation (67):

$$\text{Composite} = \beta_1 \cdot CV_1 + \beta_2 \cdot CV_2 + \ldots + \beta_n \cdot CV_n,$$

where CV_i is the standardized coefficient of variation of a trait i, β_i represents the estimated fixed-effect coefficient, and n is the number of traits included in the analyses (N=9). Mathematically, the composite is therefore the linear predictor of the morphology block, excluding the intercept. It should be interpreted as a re-parameterization of the multidimensional morphological information into a single axis, not as an independent source of information. Higher values

indicate guilds whose trait variation is aligned with the combination of morphological dimensions most strongly associated with higher relative guild richness.

To evaluate whether our conclusions depended on this dimensional reduction, we compared models including the composite with otherwise identical models including all trait-specific CVs jointly. Model fit and variance partitioning were virtually the same in both cases, indicating that the composite improved parsimony and presentation without changing the ecological interpretation.

supplementary text 10: autocorrelation in analyses of BBS routes in North America

We performed two sensitivity analyses to consider potential spatial and temporal autocorrelation. Regarding to potential spatial autocorrelation, each spatial unit (i.e., BBS route) is represented multiple times in the dataset—once for each trophic guild—meaning that observations from the same location are not spatially comparable in the usual sense. In standard spatial models, geographic proximity is typically assumed to indicate ecological similarity in the response variable (e.g., Tobler's first law (83)). However, in our case, multiple observations from the same site (i.e., with distance = 0) represent different trophic guilds, which are biologically distinct and may vary substantially in richness. Thus, spatial proximity between observations does not necessarily imply ecological similarity in the variable being modelled. We partly addressed spatial autocorrelation including a random intercept effect of route (individual BBS transect) nested within states (largest administrative unit below country) in these model. A more rigorous approach would involve a custom spatial covariance matrix that links only observations from the same trophic guild across different locations, while excluding spatial dependencies between different guilds within the same location. This approach is analytically and computationally intractable for our dataset, which comprises 164,267 observations. However, to further evaluate the robustness of our findings to potential spatial autocorrelation, we conducted a complementary sensitivity analysis based on spatial rarefaction. Specifically, for each year between 1997 and 2022, we repeated the analysis 100 times, each time selecting a single random BBS route per province. We then recalculated the models and averaged the resulting $R^2_{marginal}$ values across repetitions. This procedure reduced spatial redundancy and limited the influence of spatial clustering within regions. Results remained virtually unchanged ($R^2_{marginal}$ = 0.88±0.01; mean ± s.d.), demonstrating that our findings are not driven by spatial structure of the data. We also conducted a blocked cross-validation in which entire states were held out from model fitting and used only for prediction (supplementary text 8).

To account for potential temporal autocorrelation in the data, we repeated our analysis separately for each year from 1997 to 2022. This year-by-year approach allowed us to test whether our results were consistent over time, independent of any underlying temporal structure. Each annual model included the same fixed effects and random effects as above. Across the annual models, the $R^2_{marginal}$ was consistent with the main results ($R^2_{marginal}$ = 0.877±0.005; mean ± s.d.). The relationship of the three predictors were qualitatively similar to that observed in the joint analyses (estimate ± s.e. for total guild biomass = 0.211 ± 0.004, for individuals per unit biomass = 0.181 ± 0.004, and for morphological diversity = 0.349 ± 0.004; all $p < 0.001$). These results support that the high explanatory power is not related to any temporal structure of the data.

supplementary text 11: Propagating uncertainty in species density estimates

Santini et al. (31) provided predictions of global species-level average densities together with their associated uncertainty. In addition, density values for species without available predictions were imputed with uncertainty, as described in supplementary text 16. To evaluate whether uncertainty in species density estimates affected our ecological inference, we propagated this uncertainty through the full global analysis using a Monte Carlo approach. We repeated the analysis 100 times. In each iteration, we drew one density value per species from a normal distribution on the log10 density scale, defined by the estimated mean density and its associated uncertainty (supplementary text 16). In each iteration, we recalculated total guild biomass, individuals per unit biomass and performed the full mixed-effects model.

Results were highly consistent across uncertainty iterations. The full model explained a substantial proportion of variation in relative guild richness (mean $R^2_{marginal}$=0.583, 95% percentile interval = 0.573–0.591). All three predictors were positively associated with relative guild richness in every iteration. Morphological diversity showed the strongest standardized effect (mean estimate ± mean s.e. = 0.307 ± 0.001; 95% percentile interval for the estimate = 0.294–0.322), followed by total guild biomass (0.211 ± 0.001; 0.192–0.228) and individuals per unit biomass (0.068 ± 0.001; 0.053–0.082). All $p < 0.001$ in all 100 iterations.

Overall, propagating uncertainty in global density predictions (31) did not alter the main ecological inference: guilds with greater morphological diversity, greater total biomass and more individuals per unit biomass tended to contain a higher relative richness of species.

supplementary text 12: Measuring morphological diversity as the mean pairwise distance among species in large-scale bird assemblages worldwide

As an alternative to our composite variable based on coefficients of variation, we quantified morphological diversity within each trophic guild as the mean pairwise distance (MPD) among species in a multivariate trait space. We used the same nine morphological traits considered in the main global analyses. Traits were $\log_{10}$-transformed and standardized to mean 0 and standard deviation 1 across all species retained in the global analysis. For each trophic guild within each grid cell, MPD was calculated as the mean Euclidean distance among all species pairs. Guilds represented by a single species were assigned an MPD of 0. We then repeated the same global cell-level analysis used in the main text, replacing only the proxy for morphological diversity. Our results were consistent with the main global analysis. More speciose guilds showed higher mean pairwise morphological distance, greater total guild biomass and more individuals per unit biomass (estimate ± s.e. = 0.205 ± 0.001, 0.298 ± 0.001, and 0.201 ± 0.001, respectively; all *P* value < 0.001; ($R^2_{marginal}$= 0.527). As in the local-scale analysis, our ecological inference was robust to alternative proxies of diversity in foraging strategies and niche partitioning.

supplementary text 13: Measuring species energetic demand as the median metabolic basal rate in large-scale bird assemblages worldwide

We performed a sensitivity analysis to assess whether our inferences in the large-scale analyses depended on energetic predictors calculated from global estimates of species-level densities. Because total guild biomass requires abundance or density information, we excluded this variable from this sensitivity analyses. However, we replaced the predictor individuals per unit biomass with the median basal metabolic rate (BMR) per guild. For each species, we calculated the BMR as an allometric function of adult body mass (64, 65): $BMR_i = M_i^{0.67}$, where BMR_i is the basal metabolic rate proxy of species *i*, and M_i is the mean adult body mass of species *i*. This proxy assumes that energetic demand scales allometrically with body size, so larger-bodied species are expected to have higher per-individual energetic requirements. For each grid cell and trophic guild, we calculated the median BMR_i across all species belonging to that guild. We used the median rather than the mean to reduce the influence of exceptionally large-bodied species within guilds. We then repeated the same model specification as in the main analyses, but excluding total guild biomass and replacing individuals per unit biomass with median guild-level BMR.

Results showed that more speciose guilds had higher morphological diversity and lower median basal metabolic rate (estimate ± s.e. = 0.420 ± 0.001 and −0.025 ± 0.001, respectively; both $p < 0.001$; $R^2_{marginal} = 0.570$). As in the local-scale analysis, our ecological inference was robust to an alternative proxy of species energetic demand.

supplementary text 14: Large-scale analyses defining bird assemblages at the level of grid cell and habitat combination

In the main large-scale analyses, bird assemblages were defined as all species co-occurring within the same equal-area grid cell. This definition aggregates species associated with different habitat types within the same grid cell. For example, forest, grassland, wetland and rocky habitats can occur within a single 110 × 110 km grid cell, and species associated with these habitats may not form a single ecologically homogeneous assemblage. We therefore performed a sensitivity analysis in which global assemblages were redefined at a finer ecological grain, treating each grid cell × habitat combination as a separate assemblage.

To define these habitat-level assemblages, we combined information on the proportional cover of each habitat within each grid cell with species-level habitat-suitability information. Habitat cover was obtained from the global habitat raster maps of Jung et al. (72), from which we calculated the proportional extent of each habitat type within each grid cell. We then combined these habitat-cover proportions with IUCN species-level habitat associations. Species were assigned to a grid cell × habitat assemblage when they occurred in the grid cell and the corresponding habitat was classified as suitable or marginally suitable for that species. Thus, each assemblage represented the subset of species expected to co-occur within a given habitat type inside a given grid cell. Final analyses encompassed 10,683 grid cells, 50 habitats, and 106,067 unique combinations of grid cells and habitats.

For each grid cell × habitat assemblage, we recalculated trophic structure as the relative species richness of each trophic guild. We also recalculated the same three ecological predictors used in the main analysis: total guild biomass, individuals per unit biomass and the composite index of morphological diversity. Total guild biomass and individuals per unit biomass were calculated using Santini et al. (31) species-level density estimates for the species assigned to each grid cell × habitat assemblage. The morphological diversity composite was recalculated within each grid cell × habitat assemblage using the same nine morphological traits and the same coefficient-of-variation approach used in the main global analysis.

We then fitted the same full model structure as in the main analysis, modelling $\log_{10}$-transformed relative species richness as a function of morphological diversity, total guild biomass and individuals per unit biomass. Because multiple habitat assemblages can occur within the same grid cell, the model included random intercepts for both grid cell and grid cell × habitat assemblage. Models were weighted by the proportional extent of each habitat within the grid cell, so habitat types occupying larger fractions of a grid cell contributed more strongly to the fitted model. Assemblages represented by fewer than two trophic guilds were excluded from the model to avoid estimating guild-level relationships in assemblages with minimal trophic structure.

As in the main analysis, uncertainty in species-level density estimates was propagated by repeating the analysis across 100 iterations. In each iteration, species density values were sampled from their uncertainty distributions, energetic predictors were recalculated, and the full

model was refitted. We report on the median estimate across iterations, together with the 2.5% and 97.5% quantiles.

Results showed that the relationships observed in the main global analysis were maintained when assemblages were defined at the level of grid cell × habitat. More speciose guilds had greater morphological diversity related to foraging strategies, greater total guild biomass and more individuals per unit biomass (median estimate ± s.e. = 0.153 ± 0.001, 0.372 ± 0.001 and 0.204 ± 0.001, respectively; all $p < 0.001$; median $R^2_{marginal} = 0.601$). The 2.5–97.5% percentiles of the iteration-specific estimates were 0.118–0.189 for morphological diversity, 0.323–0.420 for total guild biomass, and 0.169–0.247 for individuals per unit biomass; the corresponding percentiles for $R^2_{marginal}$ were 0.583–0.621. Thus, our ecological inference was robust to defining global assemblages at a finer ecological grain that accounts for habitat heterogeneity within grid cells.

We performed a complementary sensitivity analysis to consider that assemblages containing only few trophic guilds provide little information on relative trophic structure Specifically, we repeated the habitat-explicit analysis after retaining only assemblages represented by at least two, three, four or five trophic guilds. This allowed us to test whether the results were robust to excluding assemblages with few trophic guilds. Due to computational limitations, for this threshold analysis, we calculated total guild biomass and individuals per unit biomass, by using the central point estimates provided by Santini et al. (31), rather than propagating uncertainty in species-level density estimates across iterations. For each minimum-guild threshold, we recalculated the same three predictors used in the main analysis: the morphological diversity composite, total guild biomass and individuals per unit biomass. We then fitted the same weighted mixed-effect model, with $\log_{10}$-transformed relative guild richness as the response variable and random intercepts for grid cell and grid cell × habitat assemblage.

The number of retained grid cell × habitat assemblages decreased from 100,787 under the ≥2-guild threshold to 76,703 under the ≥5-guild threshold. Across all thresholds, the associations between guild relative richness and the three ecological predictors were consistent with the main analysis. More speciose guilds showed higher morphological diversity, greater total guild biomass and more individuals per unit biomass (table S4). The full model explained 55.7% of the variation in relative guild richness when retaining assemblages with at least two trophic guilds, increasing to 62.2% when retaining only assemblages with at least five trophic guilds (table S4).

Minimum guilds	N cell x habitat assemblages	N grid cells	N habitats	Morphological diversity (estimate ± s.e.)	Total guild biomass (estimate ± s.e.)	Individuals per unit biomass (estimate ± s.e.)	$R^2_{marginal}$
>=2	100,787	10,637	44	0.0037 ± 0.0004	0.570 ± 0.0004	0.362 ± 0.0003	0.557
>=3	96,508	10,589	42	0.0039 ± 0.0004	0.568 ± 0.0004	0.362 ± 0.0003	0.569
>=4	90,230	10,507	40	0.0039 ± 0.0004	0.565 ± 0.0004	0.363 ± 0.0004	0.588
>=5	76,703	10,232	38	0.0035 ± 0.0004	0.568 ± 0.0005	0.367 ± 0.0004	0.622

Table S4. Habitat-explicit sensitivity analyses of the association between guild relative richness and ecological predictors. Assemblages were defined as grid cell × habitat combinations and filtered to retain only assemblages containing at least the indicated minimum number of trophic guilds. The N cell × habitat assemblages column indicates the number of retained grid cell × habitat combinations; N cells and N habitats indicate the number of unique grid cells and habitat classes represented after filtering. This analysis used central point estimates of model predictions (supplementary text 16) when calculating total guild biomass and individuals per unit biomass, without propagating density uncertainty across iterations. Estimates are standardized slopes +/- s.e. for the morphological diversity composite, total guild biomass and individuals per unit biomass. For both predictors, all $p < 0.001$. $R^2_{marginal}$ corresponds to the full weighted mixed-effect model and represents the variance explained by the three fixed effects.

supplementary text 15: Alternative dietary classifications in global analyses

We assessed whether the strong global similarity in trophic structure depended on the dietary classification used in the main analysis. To do so, we repeated the global similarity analysis using two alternative representations of assemblage trophic structure based on EltonTraits dietary data (9).

First, we reassigned species to trophic guilds using the same EltonTraits-based rule described for the local-scale sensitivity analysis in supplementary text 1. Briefly, species were assigned to the resource category that accounted for more than half of their diet, equivalent to ≥60% given the 10% resolution of EltonTraits, and species without a dominant resource category were classified as omnivores. We then recalculated the relative species richness of EltonTraits-based guilds in each global grid-cell assemblage and fitted the same global similarity model used in the main analysis, with relative guild richness modelled as a function of guild identity and grid cell included as a random intercept.

Second, we used a continuous resource-based representation of trophic structure to avoid assigning species with mixed diets to single discrete guilds. For each grid cell, we summed the EltonTraits dietary proportions of all species present across the eight resource categories—invertebrates, terrestrial vertebrates, fish, carrion, fruits, nectar, seeds and other plant material—and divided each resource total by the summed diet total of the assemblage. This produced, for each grid cell, a continuous dietary profile describing the average proportional use of each resource by the species present. We then fitted an equivalent global similarity model in which proportional resource use was modelled as a function of resource identity, with grid cell included as a random intercept.

Both analyses supported the same conclusion as the main analysis. Assemblages showed strong global similarity when trophic structure was represented using EltonTraits-based categorical guilds ($R^2_{marginal}$=0.89) and when represented as continuous resource-use profiles ($R^2_{marginal}$=0.92). Thus, the inference that bird assemblages worldwide share a strongly convergent trophic structure does not depend on the AVONET trophic-guild classification or on forcing species with mixed diets into discrete categories.

supplementary text 16: Construction and validation of global density-based energetic predictors

Santini et al. (31) provided broad species-level predictions of average density for 9,089 species, not to estimate local variation across species and grid cells. To perform the analyses, we first harmonized taxonomy across the global density dataset, bird distribution maps, and morphological data using the BirdLife–BirdTree crosswalk provided by Tobias et al. (10), which relates the names from both databases. After harmonization, Santini et al. density estimates were available for 8,047 of the 8,648 species retained in the global assemblage dataset: 6,618 exact-name matches and 1,429 crosswalk matches. The remaining 601 species were assigned density estimates using a hierarchical imputation procedure based on body mass and taxonomy. Missing values were predicted using genus + mass whenever possible, then family + mass, then order + mass, and finally a global mass-only model. In the final pipeline, 320 species were imputed using genus + mass, 41 using family + mass, 161 using order + mass, and 79 using the global mass-only model. We evaluated the imputation procedure by repeated cross-validation. As expected, predictive error increased as taxonomic information became coarser. Approximate multiplicative prediction error was 1.37-fold for genus + mass imputations, 1.44-fold for family + mass, 1.56-fold for order + mass, and 1.65-fold for the global mass-only model. For comparison, the original density-based estimates database retained in our dataset carried broad propagated uncertainty, with a median multiplicative uncertainty of 3.29-fold. These two quantities are not identical: one measures how well our imputation models predict missing densities, whereas the other measures how uncertain the original density estimates already are. Even so, the comparison shows that our imputations do not introduce a qualitatively larger level of uncertainty. Propagating this uncertainty in analyses yielded similar results (supplementary text 11).